JOURNAL OF GEOPHYSICAL RESEARCH, VOL. 102, NO. B8, PAGES 18,013–18,033, AUGUST 10, 1997

Southern California Permanent GPS Geodetic Array: Continuous measurements of regional crustal deformation between the 1992 Landers and 1994 Northridge earthquakes

Y. Bock,[1] S. Wdowinski,[1,2] P. Fang,[1] J. Zhang,[1] S. Williams,[1] H. Johnson,[1] J. Behr,[1]
J. Genrich,[1] J. Dean,[1] M. van Domselaar,[1,3] D. Agnew,[1] F. Wyatt,[1] K. Stark,[1]
B. Oral,[1] K. Hudnut,[4] R. King,[5] T. Herring,[5] S. Dinardo,[6] W. Young,[7]
D. Jackson,[8] and W. Gurtner[1,9]

Abstract. The southern California Permanent GPS Geodetic Array (PGGA) was established in 1990 across the Pacific-North America plate boundary to continuously monitor crustal deformation. We describe the development of the array and the time series of daily positions estimated for its first 10 sites in the 19-month period between the June 28, 1992 (M_W=7.3), Landers and January 17, 1994 (M_W=6.7), Northridge earthquakes. We compare displacement rates at four site locations with those reported by *Feigl et al.* [1993], which were derived from an independent set of Global Positioning System (GPS) and very long baseline interferometry (VLBI) measurements collected over nearly a decade prior to the Landers earthquake. The velocity differences for three sites 65-100 km from the earthquake's epicenter are of order of 3-5 mm/yr and are systematically coupled with the corresponding directions of coseismic displacement. The fourth site, 300 km from the epicenter, shows no significant velocity difference. These observations suggest large-scale postseismic deformation with a relaxation time of at least 800 days. The statistical significance of our observations is complicated by our incomplete knowledge of the noise properties of the two data sets; two possible noise models fit the PGGA data equally well as described in the companion paper by *Zhang et al.* [this issue]; the pre-Landers data are too sparse and heterogeneous to derive a reliable noise model. Under a fractal white noise model for the PGGA data we find that the velocity differences for all three sites are statistically different at the 99% significance level. A white noise plus flicker noise model results in significance levels of only 94%, 43%, and 88%. Additional investigations of the pre-Landers data, and analysis of longer spans of PGGA data, could have an important effect on the significance of these results and will be addressed in future work.

Introduction

The southern California Permanent GPS Geodetic Array (PGGA) was established in the spring of 1990 to evaluate continuous Global Positioning System (GPS) measurements as a new tool for monitoring crustal deformation [*Bock et al.*, 1990; *Bock and Shimada*, 1990; *Bock*, 1991; *Lindqwister et al.*, 1991]. Southern California is an ideal location because of the relatively high rate of tectonic deformation, the high probability of intense seismicity, the long history of conventional and space geodetic measurements, and the availability of a well developed infrastructure to support continuous operations. Within several months of the start of regular operations, the PGGA recorded far-field coseismic displacements induced by the June 28, 1992 (M_W=7.3), Landers earthquake [*Blewitt et al.*, 1993; *Bock et al.*, 1993a], the largest magnitude earthquake in California in the past 40 years and the first one to be recorded by a continuous GPS array. Only nineteen months later, on 17 January 1994, the PGGA recorded coseismic displacements [*Bock*, 1994] for the strongest earthquake to strike the Los Angeles basin in two decades, the (M_W=6.7) Northridge earthquake. At the time of the Landers earthquake, only seven continuous GPS sites were operating in southern California; by the beginning of 1994, three more sites had been added to the array. However, only a pair of sites were situated in the Los Angeles basin. The destruction caused by the Northridge earthquake spurred a fourfold increase in the number of continuous GPS sites in southern California within 2 years of this event. The PGGA is now the regional component of the Southern California Integrated GPS Network (SCIGN), a major ongoing densification of continuous GPS sites (Figure 1), with a

[1]Cecil H. and Ida M. Green Institute of Geophysics and Planetary Physics, Scripps Institution of Oceanography, La Jolla, California.
[2]Now at Department of Geophysics and Planetary Sciences, Tel Aviv University, Ramat Aviv, Israel.
[3]On leave from Faculty of Aerospace Engineering, Delft University of Technology, Delft, Netherlands.
[4]U.S. Geological Survey, Pasadena, California.
[5]Department of Earth, Atmospheric and Planetary Sciences, Massachusetts Institute of Technology, Cambridge.
[6]Jet Propulsion Laboratory, Pasadena, California.
[7]Riverside County Flood Control and Water Conservation District, Riverside, California.
[8]Department of Earth and Space Sciences, University of California, Los Angeles.
[9]On leave from Astronomical Institute, University of Bern, Bern, Switzerland.

Paper number 97JB01379.
0148-0227/97/97JB-01379$09.00

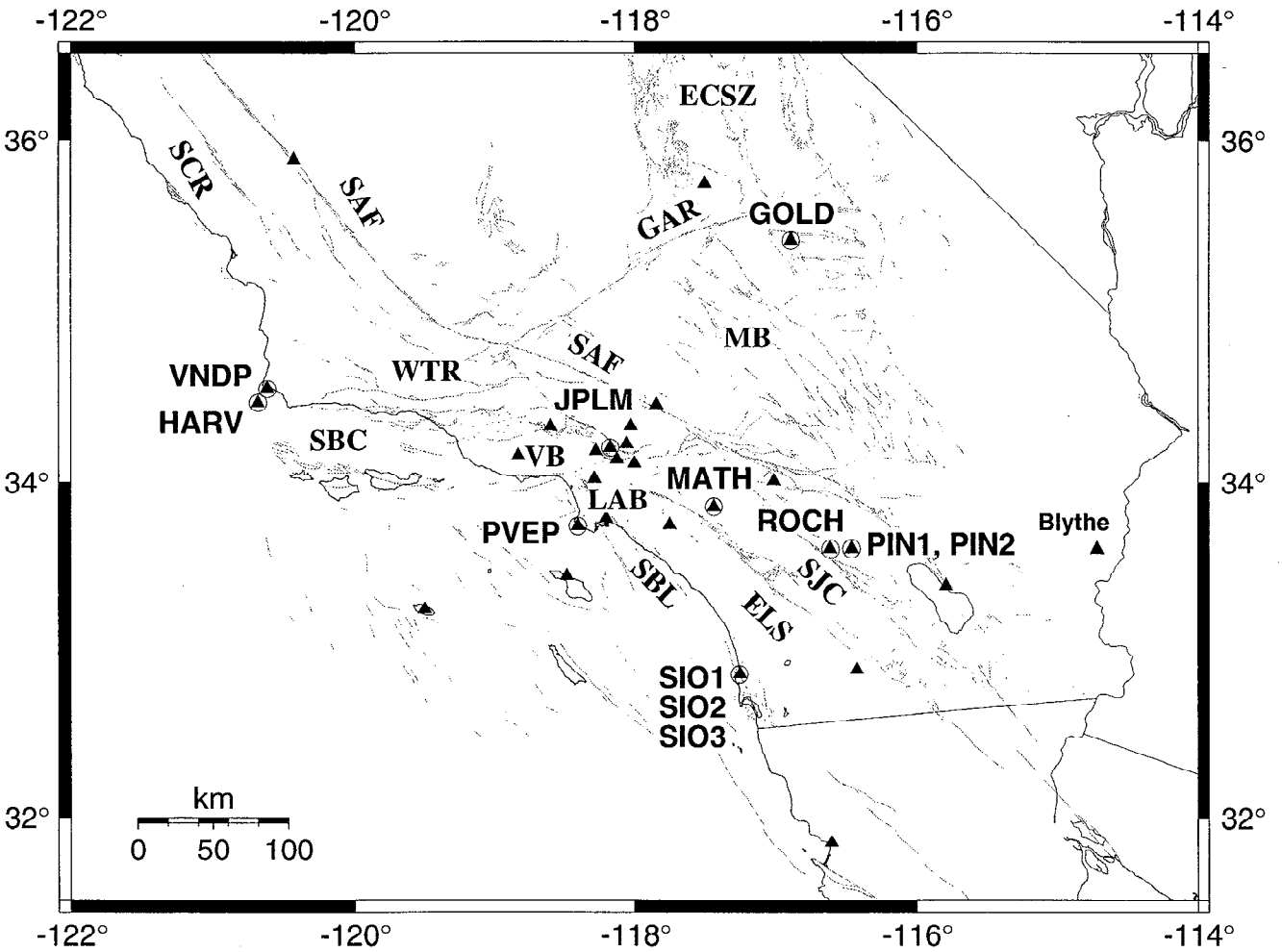

Figure 1. Sites of the Southern California Integrated GPS Network (SCIGN) circa mid-1996. The regional PGGA sites discussed in this paper are denoted by circumscribed triangles and their four-character codes. Other SCIGN sites are denoted by triangles only. Tectonic features: ECSZ, Eastern California Shear Zone; ELS, Elsinore fault; GAR, Garlock fault; LAB, Los Angeles basin; MB, Mojave Block; SAF, San Andreas fault; SBC, Santa Barbara Channel; SBL, Southern Borderlands; SCR, Southern Coast Ranges; SJC, San Jacinto fault; VB, Ventura basin; WTR, Western Transverse Ranges.

concentration in the Los Angeles metropolitan region [*Prescott,* 1996].

In a significant parallel development, a global network of continuous GPS tracking stations, under the aegis of the International GPS Service for Geodynamics (IGS) (Figure 2), became operational only several weeks before the Landers earthquake [e.g., *Beutler et al.*, 1993], providing access to a consistent global terrestrial reference frame and data for the computation of precise satellite ephemerides and Earth orientation. The IGS/PGGA synergism provides a rigorous way of computing positions of regional sites with respect to a global reference frame [*Blewitt et al.*, 1993; *Bock et al.*, 1993a], rather than the traditional approach of computing intraregional relative site positions (baselines). It then becomes possible to position one or more roving GPS receivers with respect to the regional anchor provided by a continuous GPS array, so that logistically complex field campaigns with many receivers are no longer necessary for monitoring crustal deformation [*Bevis et al.*, 1997]. Furthermore, continuous arrays are able to generate other classes of geophysical information, for example, integrated water vapor [e.g., *Bevis et al.*, 1992; *Duan et al.*, 1996] and ionospheric disturbances [*Calais and Minster*, 1995].

Continuous GPS provides temporally dense measurements of surface displacements induced by crustal deformation processes including interseismic, coseismic, postseismic, and aseismic deformation and the potential for detecting anomalous events such as preseismic deformation and interseismic strain variations. Although strain meters yield much higher short-term resolution to a period of about 1 year [e.g., *Wyatt et al.*, 1994], a single continuous GPS site is significantly less expensive than a single strain meter and probably has better long-term stability beyond a 1-year period. Compared to less frequent field measurements, continuous GPS provides the means to better characterize the errors in GPS position measurements and thereby obtain more realistic estimates of derived parameters such as site velocities.

In this and two companion papers by *Wdowinski et al.* [this issue] and *Zhang et al.* [this issue] we analyze the tectonic signals recorded in two subsets of PGGA data from the first 10 sites in the array: the 100-day position time series centered on

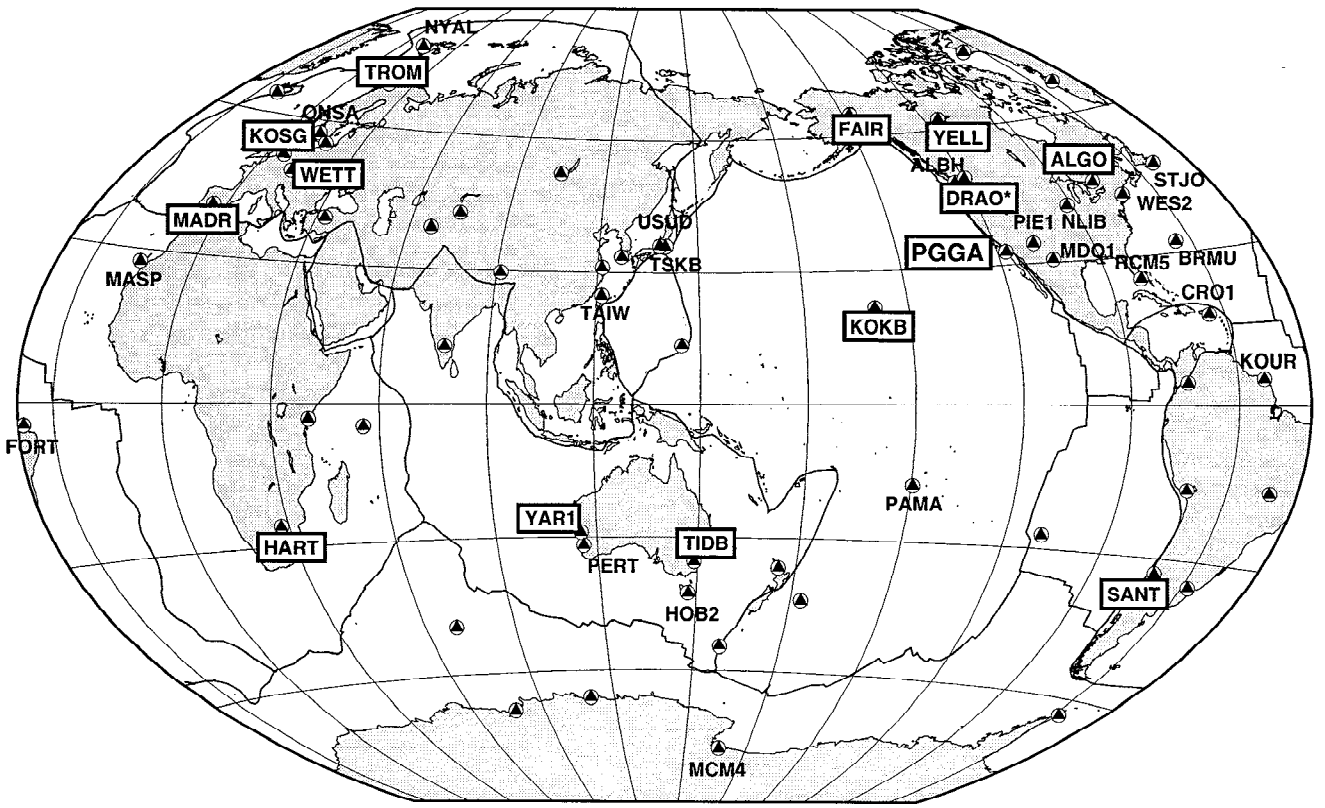

Figure 2. Global tracking sites of the International GPS Service for Geodynamics (IGS) circa mid-1996. Sites active during the period described in this paper are denoted by their four-character site code. Constraining the coordinates and velocities of the 13 IGS "core" sites (site codes enclosed in rectangles) provides access to the International Terrestrial Reference Frame 1993 (ITRF93). We have substituted DRAO for the core site GOLD in our analysis.

June 28, 1992, is examined for coseismic and short-term postseismic deformation associated with the Landers earthquake, and the 19-month series collected between the Landers and Northridge earthquakes is examined for possible changes in displacement rates after a major earthquake. Wdowinski et al. present a method to filter raw time series in order to better estimate positions of regional stations on a site by site basis and apply it to the 100-day time series. Zhang et al. analyze the stochastic properties of daily GPS position measurements in the 19-month period in order to estimate realistic site velocity uncertainties. In this paper, we describe the development of the PGGA, the components of the system developed to collect and analyze data every 24 hours, and the time series of daily positions estimated for the array's first 10 sites in the interval between the two earthquakes. We then compare site velocities fit by linear regression to these data with those estimated independently from nearly 10 years of less frequent GPS and very long baseline interferometry (VLBI) measurements [e.g., *Ryan et al.*, 1993], and address the question of whether displacement rates in southern California changed significantly at the time of the Landers earthquake.

Crustal Deformation in Southern California

Tectonic Setting

The tectonics of California are dominated by about 50 mm/yr of transcurrent motion between the Pacific and the North America plates. Unlike some other plate boundaries, which are characterized by narrow zones of deformation, the Pacific-North America boundary is diffuse with the zone of deformation 800 km wide. The deformation is localized, however, along several geologic-tectonic elements (Figure 1); the most prominent feature is the San Andreas fault zone (SAFZ) which accommodates a large part (~35 mm/yr, ~70%) of the right-lateral motion between the two plates in central and southern California. The San Andreas fault (SAF) is the primary feature of this zone of deformation. The orientation and rate of displacement vary along this fault and reflect the complex pattern of deformation in the region. Current best estimates of slip rates on the central and southern segments of the SAF range from 34±5 mm/yr on the central segment [*Working Group on California Earthquake Probabilities*, 1995] to 18–20 mm/yr at its southernmost end [*Savage et al.*, 1979]. The remainder of the SAFZ motion and Pacific/North America transcurrent plate motion is accommodated by other faults which trend roughly parallel to the SAF. In central and southern California, 12 mm/yr is absorbed to the east by the Eastern California Shear Zone [*Savage et al.*, 1990], site of the 1992 Landers earthquake. To the west, other faults including the San Jacinto, Whittier-Elsinore, Newport-Inglewood, Palos Verdes, and offshore San Clemente faults accommodate the remaining 30% of right-lateral motion.

Many aspects of the complex deformation pattern of southern California are related to the trend change ("big bend") of the SAF from a NW direction parallel to the plate motion to

a more westerly trend, making an angle of about 30° with the plate motion. The Western Transverse Ranges (WTR) are located south of the big bend and are characterized by E-W striking thrust faults and associated folds. Geologically derived estimates of convergence across the WTR indicate 18–27 mm/yr N-S shortening, with a strong component of regional uplift [*Namson and Davis*, 1988]. South of the WTR are located several basins, some of which are heavily populated. The Ventura basin is an E-W sedimentary basin (100 km long and 10–15 km wide) that is subjected to N-S shortening of 5–8 mm/yr [*Donnellan et al.*, 1993]. The Los Angeles basin (nearly 100 km wide) is contracting at a minimum rate of 4–7 mm/yr (over the last 2 m.y.) in a direction perpendicular to the SAF, for a line from Palos Verdes to the fault [*Davis et al.*, 1989]. The orientation of these rates is taken to be parallel to the line of their cross section, which is normal to the dominant structural grain as evidenced by fold axes and thrust fault trends. Recent geodetic results indicate a contraction rate of 6 ± 1 mm/yr [*Shen et al.*, 1996].

Geodetic Measurements and the Crustal Deformation Cycle

The interseismic, coseismic, and postseismic stages of the earthquake loading cycle [*Scholz*, 1990] have all been directly observed, although barring the coseismic phase, not well understood [e.g., *Thatcher*, 1984; *Wyatt et al.*, 1994]. A complete earthquake cycle, however, has yet to be observed in southern California. The earthquake loading cycle was first recognized and explained in terms of elastic rebound theory by *Reid* [1910, 1913] based on repeated triangulation surveys in California [*Hayford and Baldwin*, 1907] and Sumatra [*Müller*, 1895], inaugurating nearly a century of geodetic measurements of crustal deformation. In California, repeated triangulation measurements were initiated by the U.S. Coast and Geodetic Survey in response to the 1906 San Francisco earthquake. These surveys conducted about once every 10 years yielded the first estimates of crustal motion [*Bowie*, 1928; *Whitten*, 1955; *Thatcher*, 1979].

An extensive series of trilateration surveys (electronic distance measurements) was performed in California by the U.S. Geological Survey over a 20-year period beginning in the early 1970s to determine the regional velocity field in more detail and to detect potential temporal changes in the rate of deformation [*Savage et al.*, 1986]. Analyses of trilateration and older triangulation data fail to provide evidence for variations in interseismic deformation rates [e.g., *Lisowski et al.*, 1991; *Savage*, 1995; *Savage and Lisowski*, 1995a]. *Savage and Lisowski* [1995b], relying on frequent distance measurements several years before and after two nearby earthquakes, the 1984 Morgan Hill and 1989 Loma Prieta earthquakes, argue that the postseismic rate differed from the preseismic rate for at least one of the lines examined. Such phenomena have been difficult to detect, however, since potential signals might be aliased due to infrequent sampling associated with these types of data, and any longer wavelength (>20 km) signals could be missed.

GPS, interferometric synthetic aperture radar (INSAR), and strain meters have become the most widespread geodetic methods presently in use for measuring crustal deformation. In southern California, coseismic deformation has been observed with GPS for the 1987 Superstition Hills sequence (M_S=6.2, 6.6) [*Larsen*, 1990], the 1992 Joshua Tree (M_W=6.1) [*Bennett et al.*, 1995], the 1992 (M_W=7.3) Landers [*Blewitt et al.*, 1993; *Bock et al.*, 1993a; *Miller et al.*, 1993, *Freymueller et al.*, 1994], and the 1994 (M_W=6.7) Northridge earthquakes [e.g., *Bock*, 1994; *Hudnut et al.*, 1996], and by INSAR for the Landers [*Massonnet et al.*, 1993, 1994; *Zebker et al.*, 1994] and Northridge [*Massonnet et al.*, 1996a; *Murakami et al.*, 1996] earthquakes.

Significant postseismic deformation was observed following the (M_S=7.1) Loma Prieta earthquake from frequent GPS field surveys extending to 3.3 years after the event [e.g., *Savage et al.*, 1994; *Burgmann et al.*, 1997], and for the Landers earthquake by laser and borehole strainmeters [*Wyatt et al.*, 1994; *Johnston et al.*, 1994], field GPS surveys [*Shen et al.*, 1994; *Savage and Svarc*, 1997], continuous GPS measurements [*Wdowinski et al.*, 1992, this issue], and INSAR [*Massonnet et al.*, 1996b; *Peltzer et al.*, 1996]. In addition, *Heki et al.* [1997] observed postseismic deformation following the December 28, 1994 (M_W=7.6), Sanriku-Haruka-Oki earthquake located off the Senriku coast, northeastern Japan. This transient signal differs from those mentioned above in that it is due to an interplate thrust earthquake, total postseismic displacements a year after the event are nearly as large as the coseismic displacements, and the deformation occurs over a relatively large area.

A preseismic phase in the earthquake cycle is more elusive, and its existence is only suggested by fragmentary observations of anomalous crustal deformation prior to large earthquakes [*Scholz*, 1990]. Preseismic deformation in the days to minutes before an earthquake have not been detected in California by strain and tilt measurements, including the 1992 Landers earthquake [*Wyatt et al.*, 1994; *Johnston et al.*, 1994]. However, *Gladwin et al.* [1991] reported a change in deformation rate about a year before the 1989 Loma Prieta earthquake detected by borehole strainmeters.

Continuous Geodetic Measurements

Seismic networks provide temporally and spatially dense measurements of very short term ground motions generated by seismic waves. They provide detailed information on fault geometry but are insensitive to slower fault motion. Slow fault motions can only be detected from the quasi-static deformations which they cause and are observable from surface (or near-surface) strain or tilt measurements. Since these deformations decay with distance from the source as r^{-3}, compared to r^{-2} for seismic waves, instruments need to be located relatively close to the earthquake epicenter or a fault surface [*Wyatt et al.*, 1994]. Laser and borehole strain meters make essentially point measurements of near-surface strain with very high short-term accuracy, about 3 orders of magnitude better than other geodetic methods. However, they are expensive (as evidenced by their sparse coverage in California) and can lack very long-term stability.

Continuous GPS is another method for obtaining frequent measurements of crustal deformation, providing estimates of station position with a Nyquist frequency potentially as high as one-over several minutes (more often one-over two days) and, by repeated measurements, estimates of surface displacements. Although strain meters yield much higher short-term resolution, continuous GPS is significantly less expensive and may have better long-term stability beyond a period of about 1 year. Furthermore, unlike campaign-mode GPS measurements, continuous GPS provides the temporal resolution required to better characterize the GPS error

spectrum [*King et al.*, 1995], and to assign more realistic uncertainties to derived crustal motion quantities such as site velocities [*Zhang*, 1996; *Zhang et al.*, this issue] and coseismic displacements [*Wdowinski et al.*, this issue].

The first continuous GPS network was established in 1988 in the Kanto-Tokai region of central Japan [*Shimada et al.*, 1989]. In July 1989, this network recorded a precursory signal to an underwater volcanic eruption [*Shimada et al.*, 1990; *Okada and Yamamoto*, 1991]. *Shimada and Bock* [1992] interpreted interseismic deformation patterns in the Kanto plain and Izu Peninsula based on 17 months of semiweekly observations from this network. In 1990, the first four stations of the PGGA were established; today more than 45 stations are operational in southern California (Figure 1). Additional regional continuous GPS networks have been introduced subsequently to monitor crustal deformation in, for example, western Canada [*Dragert and Hyndman*, 1995], northern California [*King et al.*, 1995], Japan [*Tsuji et al.*, 1995], and Scandinavia [*Jaldehag et al.*, 1996].

Description of the Array

Site Selection

The PGGA spans most of the important tectonic elements in southern California between the Pacific plate and stable North America (Figure 1). The westernmost site on the Pacific coast, at Vandenberg Air Force Base (VNDP), is located 150 km west of the SAF and moves within 1–2 mm/yr of the rate of the Pacific plate [*Ward*, 1990; *Feigl et al.*, 1993]. Similarly, Blythe (BLYT), the easternmost site, lies about 100 km east of the SAF and is assumed to move with the North America plate [*Bennett al.*, 1995]. The remainder of the sites are located within the zone of deformation between the Pacific coast and the Mojave Block (Figure 1). Initial siting was determined according to three criteria: logistics, distance between sites, and coverage of significant tectonic elements. Logistical constraints included local geological setting, a secure facility, a power source, reliable communication links, good sky visibility, and low multipath environment. Initial intersite spacing in the range of 100–400 km allowed coverage of the plate boundary in southern California at reasonable spacing for GPS phase ambiguity resolution [*Dong and Bock*, 1989]. Tectonic elements of initial concern were the major faults (SAF, San Jacinto, and Elsinore) and the densely populated Los Angeles basin.

The initial station deployments were a compromise between convenience, logistics, and the goal of regional spatial coverage. Station SIO1 moving at close to Pacific plate velocity was conveniently located on the campus of Scripps Institution of Oceanography (SIO) in La Jolla. SIO is just northwest of the Rose Canyon fault with a slip rate of 1–2 mm/yr [*Lindvall and Rockwell*, 1995]. Station PIN1 was installed at the Piñon Flat Observatory (PFO) in Riverside County. Continuous GPS monitoring at PFO allows us to compare results with other continuous records collected by strain meters and tiltmeters at that facility. The San Jacinto fault and the southern section of the San Andreas fault lie within a distance of 25 km from PFO. The estimated rupture probabilities for the San Bernadino Valley and San Jacinto Valley segments of the San Jacinto fault are considered to be high (~40%) for the time period 1994 to 2024 [*Working Group on California Earthquake Probabilities*, 1995]. Station JPLM was located at the Jet Propulsion Laboratory near an existing geodetic mark set originally for mobile VLBI measurements. Situated within the Sierra Madre-Cucamonga fault zone, it is an important reference site for GPS surveys in the Los Angeles basin, a densely populated area at considerable seismic risk [*Dolan et al.*, 1995]. Station GOLD was already part of the NASA Deep Space Network (DSN), located at the NASA Goldstone facility within the Eastern California Shear Zone. The station VNDP at Vandenberg Air Force Base allowed continuation of an 8-year series of VLBI observations near the western edge of the plate boundary. While distances between these initial sites vary from 100 to 400 km, another pair of stations (PIN2 and ROCH) was installed 14 km apart to evaluate the continuous GPS method at a distance typical of fault dimensions [*Happer et al.*, 1991]. Site PIN2 was constructed only 50 m from PIN1, primarily to evaluate stable geodetic monument design. All seven sites experienced significant coseismic deformation during the Landers earthquake. Several months after the earthquake, additional sites were established at Lake Mathews (MATH), between the Elsinore and San Jacinto faults, as a base station for GPS field surveys in Riverside County; on the Palos Verdes Peninsula (PVEP) to form a baseline with JPLM spanning the Los Angeles basin (installed only 9 months before the Northridge earthquake); and the Harvest Oil Platform (HARV) in the Santa Barbara Channel, 11 km west of VNDP, to support satellite altimetry. The Northridge earthquake significantly displaced the two sites in the Los Angeles basin (JPLM and PVEP) [*Bock*, 1994; *Hudnut et al.*, 1996]. Additional sites (e.g., Blythe, Figure 1) became operational very late in or after the period described in this paper and are not discussed further.

The relevant site parameters for the 10 PGGA sites described in this and the two companion papers by *Zhang et al.* [this issue] and *Wdowinski et al.* [this issue] are documented in Table 1. The basic components of our data collection, analysis, and archiving system are shown in Figure 3.

Monumentation

During the selection of sites we considered site geology, but in several cases, nearby monuments had a history of space geodetic measurements from VLBI projects (JPLM, PIN1/2, PVEP, VNDP). At those sites, we decided to occupy monuments very close to the original VLBI marks. At a few sites, we could make our own choice for the location of a new monument installation (MATH, SIO, ROCH). Typically, this meant finding the best available rock in a logistically feasible location.

The sites MATH and ROCH are the only two bedrock-anchored monuments discussed in this paper. MATH is in slightly fractured basic intrusive rocks, whereas ROCH is in a large granitic outcropping of the Peninsular Ranges batholith. The monuments PIN1 and PIN2 are installed in similar granitic rock but in a location where a several meter thick layer of decomposed rock overlies bedrock. At PVEP, SIO, and VNDP, nearby coastal outcrops show highly fractured shales, and the monuments are set atop coastal terraces that were cut into these soft metasedimentary rocks. JPLM is set in the Gould mesa, an uplifted remnant of a dissected Pleistocene alluvial fan.

Several studies have shown that a lack of stable monumentation can introduce significant amounts of colored noise in geodetic observations. Because of this, stable GPS monuments were especially designed for use in the PGGA

Table 1. PGGA Site Information

Site Code	Site Name and Location	Geodetic Coordinates	Monument Description	Effective Date	Receiver Type	Firmware	Antenna Type	Antenna Height
GOLD	Goldstone, NASA Deep Space Network, Fort Irwin	35° 25' 30.56363" 116°53' 21.29388" 986.726	25 m tall, unguyed, microwave tower	April 15, 1992	R SNR-8	6.90, 7.10	DM R	0.0000*
HARV	Texaco Harvest Oil Platform, Santa Barbara Channel	34° 28' 09.83470" 120°40' 55.41903" 15.047	"Harvest GPS Pier," submarine fan	June 26, 1992	SNR 8000	1.41, 2.00, 2.20, 2.50, 2.60, 2.80	DM T	0.1000
JPLM	Gould Mesa, Jet Propulsion Laboratory, Pasadena	34° 12' 17.34782" 118°10' 23.59972" 424.046	JPL MV-3 1983, mobile VLBI marker, alluvial fan	April 14, 1992	R SNR-8	7.00, 7.20, 7.30, 7.40, 7.50, 7.80	DM R	0.0930
MATH	Lake Mathews Reservoir, Riverside County	33° 51' 24.06362" 117°26' 12.51964" 396.934	stainless steel rod (Figure 4c), intrusive rock outcrop	April 14, 1993	T SSE	5.52	4000 ST	0.7075
PIN1	Piñon Flat Observatory 1, Riverside County	33 °36' 43.75908" 116° 27' 29.36501" 1256.229	deeply anchored (Figure 4a), covered crystalline rock	April 25, 1992 Sept. 25, 1992 June 22, 1993 Nov. 6, 1993	R SNR-8 A LX-II3 R SNR-8 A ZX-II3	7.00 6M 7.30, 7.50 1B10	DM R L1/L2 P-B DM R L1/L2 P-B	1.8435
PIN2	Piñon Flat Observatory 2, Riverside County	33° 36' 43.72989" 116° 27' 27.41350" 1258.352	deeply anchored (Figure 4b), covered crystalline rock	Mar. 7, 1991	T SST	4.11	4000 ST	0.1435
PVEP	Palos Verdes, NIKE missile base, Palos Verdes Peninsula	33° 44' 36.83633" 118° 24' 15.27300" 69.436	stainless steel rod in massive concrete bunker, fractured soft rock	May 17, 1993 Oct. 26, 1993 Nov. 10, 1993	T SSE T SST T SSE	5.52 4.64 6.04	4000 ST	0.2475
ROCH	Pinemeadow , Riverside County	33° 36' 39.68278" 116° 36' 35.16382" 1393.784	stainless steel rod (Figure 4c), granitic rock outcrop	April 19, 1991 July 3, 1992	T SST	4.11	4000 ST	0.2475 0.2440
SIO1	Scripps Institution of Oceanography 1, La Jolla, San Diego County	32° 52' 03.98396" 117° 15' 08.39653" 7.562	deeply anchored (Figure 4a), fractured soft rock	April 25, 1992	R SNR-8	7.00	DM R	1.8458
SIO2	Scripps Institution of Oceanography 2, La Jolla, San Diego County	32° 52' 02.96479" 117° 15' 08.80822" 8.174	eccentric mark to SIO1 and SIO3, mount attached to hanging wall of SIO library	June 6, 1992 Jan. 19, 1993 Mar. 18, 1993 April 6, 1993 April 14, 1993 April 23, 1993	A LX-II3 T SST A LX-II3 T SST A LX-II3 TRMSSE	6M 4.62 6M 5.52 6M 5.52	L1/L2 P-B 4000 ST L1/L2 P-B 4000 ST L1/L2 P-B 4000 ST	0.0650
SIO3	Scripps Institution of Oceanography 3, La Jolla, San Diego County	32° 51' 52.92454" 117° 15' 01.45425" 34.852	deeply anchored (Figure 4a), fractured soft rock	July 9, 1993 Aug. 6, 1993 Aug. 10, 1993 Nov. 5, 1993	A LX-II3 T SST A LX-II3 A ZX-II3	7A 4.64 7A, 7B 1B10, 1B12, 1C00, 1C01	L1/L2 P-B 4000 ST L1/L2 P-B L1/L2 P-B	1.8448
VNDP	Vandenberg Air Force Base, Santa Maria basin	34° 33' 22.71125" 120° 36' 59.20146" -11.518	deeply anchored (Figure 4a), fractured soft rock	May 25, 1992 Jan. 12, 1993	A LX-II3 R SNR-8	6M 7.30, 7.40, 7.50	L1/L2 P-A DM R	1.8420 1.8480

Geodetic coordinates, north latitude, west longitude, and height (in meters) are with respect to the WGS84 ellipsoid (semimajor axis is 6,378,137.0 m; inverse flattening is 298.257222101). Receiver types are R SNR-8 , JPL Rogue SNR-8; SNR 8000, Allen Osborne Associates TurboRogue; T SST/SSE, Trimble 4000 SST/SSE; A LX-II3/ZX-II3, Ashtech LX II3/ZX-II3 (P-12/Z-12). Antenna types are DM R/T, Dorne Margolin R/T with choke rings (JPL Design/Allen Osborne Associates); 4000 ST, Trimble 4000 L1/L2 Geod; L1/L2 P-A/B, Ashtech Geodetic Rev A/B. Antenna heights (in meters) are measured vertically to the bottom of the antenna (direct height to antenna preamplifier base, DHPAB, which is the RINEX convention).

*GOLD antenna height is referenced to the top of the choke rings (TCR).

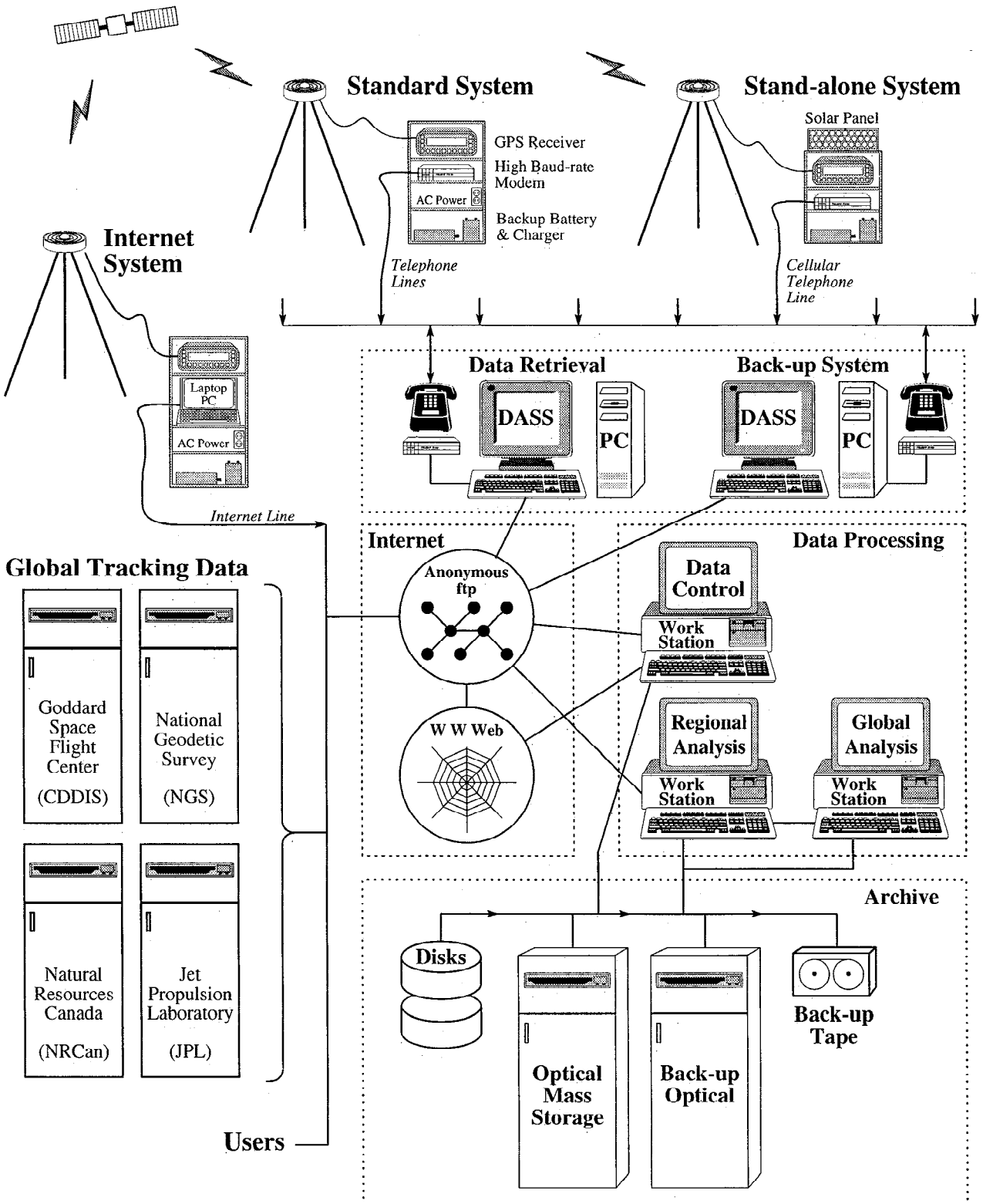

Figure 3. Schematic of continuous monitoring system developed at the Scripps Orbit and Permanent Array Center (SOPAC) for the PGGA. Shown are field system (three types), data retrieval (global and regional), data processing, and data archive components.

network [*Wyatt et al.*, 1989]. One such monument consists of two parts: (1) a ground level base that is anchored at depth (~10 m), laterally braced, and decoupled from the surface (~3 m), as much as possible; and (2) an antenna mount (~1.7 m tall) that can be precisely positioned on this base (Figure 4a). The removable antenna mount can also support other types of measurements such as leveling rods and EDM reflectors. This type of monument was constructed at PIN1, SIO1, SIO3, and

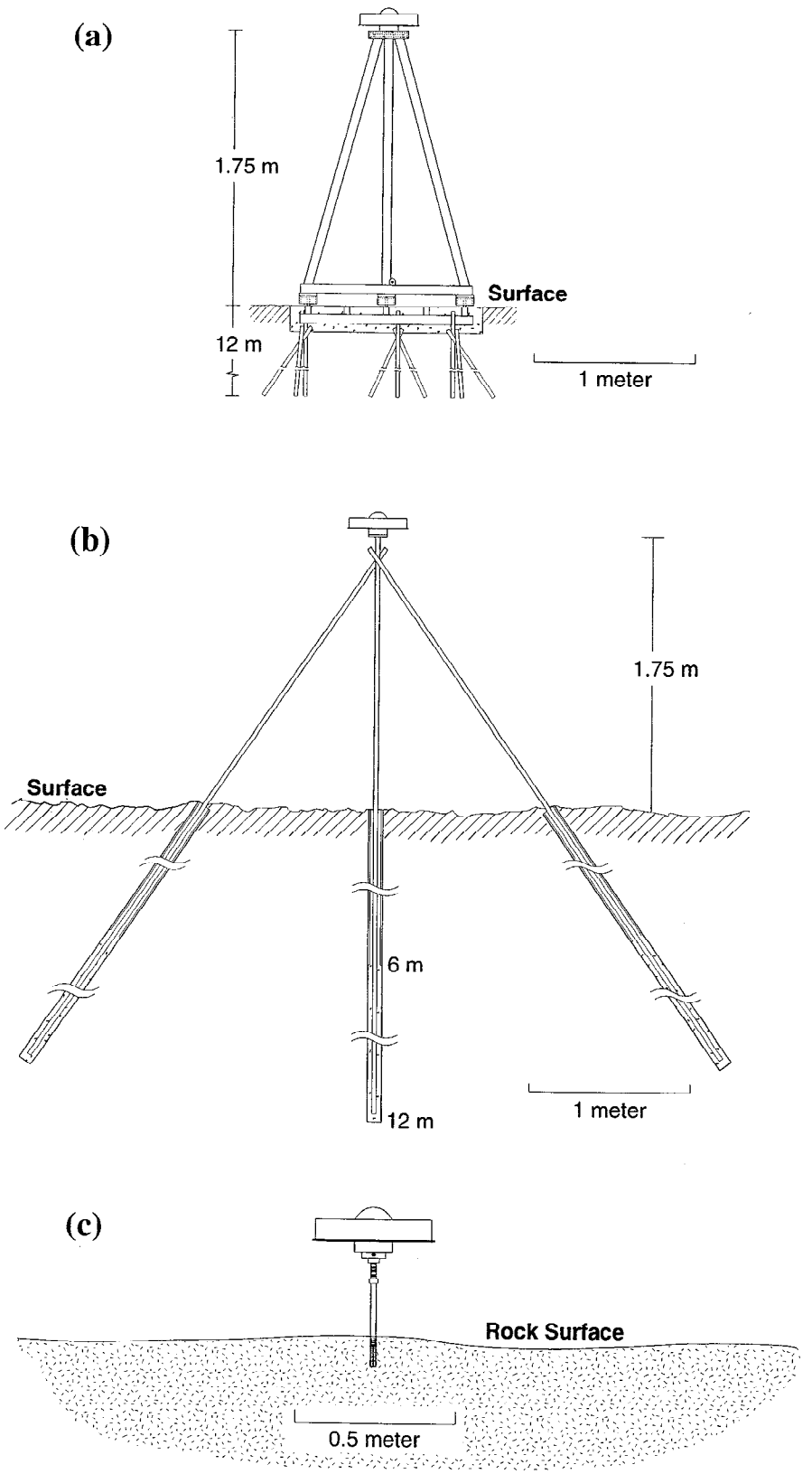

Figure 4. Monument designs for PGGA sites: (a) deeply anchored monument with concrete base and removable antenna mount, constructed at PIN1, SIO1, SIO3, and VNDP, (b) deeply anchored monument of quinqunx design, constructed at PIN2, and (c) typical bedrock anchored monument, constructed at MATH and ROCH.

VNDP. A modified version was constructed at PIN2 consisting of one vertical and four obliquely braced metal pipes anchored at depth (~10 m), decoupled from the surface, and welded together at their point of intersection about 1.5 m above the surface (Figure 4b). This type of monument was successful in attenuating seasonal displacements of two-color geodimeter reflector monuments at Parkfield, California, to less than 1 mm compared to annual variations of up to 12 mm exhibited by earlier shallow, vertically driven monuments [*Langbein et al.*, 1995]. The JPLM monument constructed originally for mobile VLBI measurements has shallower anchoring. Another strategy used to monument PGGA sites was anchoring stainless steel rods in exposed bedrock (MATH and ROCH) or massive concrete structures (PVEP) (Figure 4c). The GOLD site which sits atop a 25 m steel tower, and the HARV site, located on an offshore oil platform were not originally intended for precise crustal deformation measurements.

At the SIO site, because of unexpected construction on campus, the original mark (SIO1) was destroyed just prior to the Landers earthquake and was replaced several months later by a second permanent mark (SIO3). In the interim, an intermediate mark was occupied continuously; it is anchored to a concrete retaining wall of the SIO library (SIO2). Using local GPS surveys, the three-dimensional offsets among these three marks were computed to better than 1-mm accuracy, and a single time series "SIO3" was constructed by applying these offsets to the SIO1 and SIO2 series (Table 2).

Instrumentation

The initial hardware configuration at each of the first five sites consisted of a Rogue SNR-8 GPS receiver [*Thomas*, 1988], a rubidium oscillator, and a Dorne-Margolin antenna with choke rings. The Rogue SNR-8 receiver recorded precise phase and pseudorange ("P code") measurements at both "L1" and "L2" GPS radio frequencies, for up to eight satellites simultaneously. This capability and the multipath-reducing characteristics of the antenna assembly allowed for the efficient repair of integer cycle slips in undifferenced phase observations [*Blewitt*, 1989] and facilitated the resolution of integer-cycle phase ambiguities [*Blewitt*, 1990]. At the early stages of PGGA development receivers other than P code receivers (i.e., "L2 squaring" receivers) were deemed not suitable for near real-time operations because phase measurement cycle slip repair was too time consuming and less amenable to automatic data-editing algorithms.

While the Rogue SNR-8 receiver was the only P code receiver available at the network's inception, it had several disadvantages such as high power consumption and the need for high-level, though relatively infrequent, engineering support to keep the equipment operational. The lack of readily available support, spare parts and the implementation of "anti-spoofing" (AS) of the GPS signals by the Department of Defense resulted in occasional gaps in the otherwise continuous data series. AS significantly degraded the quality of the Rogue SNR-8 pseudorange measurements, making the phase/pseudorange combination unsuitable for cycle-slip editing and ambiguity resolution. As more advanced P code receivers became available, they were introduced into the array, particularly Ashtech Z-12 receivers, Trimble 4000 SSE receivers, and Rogue SNR 8000 (TurboRogue) receivers. These receivers are capable of measuring full-wavelength L1 and L2 phase and pseudoranges under AS conditions. Deficiencies in early firmware versions of the Ashtech P-12 receivers (deployed prior to the Z-12 receivers), as well as performance and reliability problems, resulted in gaps, particularly in some of the early data.

Table 2. SIO Site Eccentricities

	ΔX	ΔY	ΔZ
SIO1-SIO3	-65.299	267.391	271.357
SIO2-SIO3	-82.837	256.717	245.302

Global Cartesian coordinate differences. Units are meters. Offsets are applied as, for example, SIO1 (X) = SIO3 (X) + ΔX.

Communications and Data Retrieval

Remote communication with the three types of receivers in the array are over standard telephone lines (except for a cellular phone at site MATH) using 19,200 baud modems. Download and remote control software packages are provided by the manufacturer of each receiver. Receiver data are downloaded in 24-hour segments (0000–2400 UT), uncompressed, translated to the Receiver Independent Exchange Format (RINEX) [*Gurtner*, 1994], subjected to quality control analysis on scientific workstations, and transferred to archival media which are accessible via anonymous ftp (lox.ucsd.edu) and the World Wide Web (http://lox.ucsd.edu). A software package (Data Acquisition Software Suite, DASS) has been developed which controls all aspects of data manipulation including retrieval, translation, migration, quality control and archiving [*SOPAC Staff*, 1997]. A similar package has also been developed at the Jet Propulsion Laboratory [*Lindqwister et al.*, 1989].

Global Tracking and Precise Satellite Orbits

Although PGGA data have been collected since the spring of 1990, intermittent analysis actually commenced with the global GIG 1991 campaign in January 1991 [*Blewitt*, 1993] and in support of the California High Precision GPS Network (HPGN) field survey during the period of April to August 1991 [*Hudnut et al.*, 1994]. The GIG 1991 campaign, a several week deployment of a global network of Rogue SNR-8 receivers, demonstrated convincingly that P code receivers would become an important component of near real-time operational networks. By mid-1991, there were enough permanent P code receivers operating in the global network to begin computing precise ephemerides (orbits), an essential requirement for estimating small crustal motions with high accuracy. By November 1991, we were estimating daily array site positions and precise GPS satellite ephemerides within 5–7 days of data collection [*Bock et al.*, 1992; *Bock et al.*, 1993b; *Fang and Bock*, 1995]. By June 1992, several weeks before the Landers earthquake, several other groups had also begun computing precise satellite ephemerides as a pilot project for the new International GPS Service for Geodynamics (IGS) (Figure 2). The IGS was established by the International Association of Geodesy (IAG) to consolidate worldwide permanent GPS tracking networks within a single organization. Two major global networks, CIGNET [*Chin*, 1989] and the Fiducial Laboratories for Natural Science Network (FLINN) promoted by NASA [*Minster et al.*, 1989, 1991], were merged with several continental-scale networks in North America, western

Europe, and Australia. Formal operations of the IGS began in January 1994 [*Beutler et al.*, 1994].

Data Analysis

Our analysis of the PGGA and IGS data has evolved considerably since its inception, with incremental improvements being incorporated within the constraints of uninterrupted operations. The coordinate time series described here and in the companion papers by *Zhang et al.* [this issue] and *Wdowinski et al.* [this issue] are the result of a uniform reanalysis of IGS and PGGA data for the period between the Landers and Northridge earthquakes and the 100-day period spanning the Landers earthquake.

Daily Global and Regional Solutions

Oral [1994] and *Zhang* [1996] have demonstrated that combining (intersecting) global and regional solutions through an adjustment of their corresponding estimates and full covariance matrices yields parameter estimates that are statistically equivalent to a simultaneous adjustment using all the data but in a significantly more efficient manner. Our daily analysis using the GAMIT software [*King and Bock*, 1995] is based on this two-step distributed processing approach that differs from the original operational analysis at SIO; the two approaches are compared in Table 3. In the global solution, IGS data are analyzed by weighted least squares, estimating initial conditions and nongravitational force parameters for each satellite, coordinates for the global tracking stations, Earth orientation parameters, atmospheric zenith delay parameters, and carrier phase ambiguities. To increase processing efficiency, the global solution uses data sampled at a 120 s interval and does not attempt resolution of integer-cycle phase ambiguities. In the regional solution, the PGGA data are analyzed simultaneously with data from four IGS stations (Figure 2), now sampled at a 30 s interval, with constraints imposed on the orbital parameters estimated in the global solution. The same types of parameters are estimated but in a multistep approach that includes integer-cycle phase ambiguity resolution [*Dong and Bock*, 1989; *Feigl et al.*, 1993]. At the final steps of both the global and regional solutions, all estimated parameters are loosely constrained to impose only a very weak reference frame [*Feigl et al.*, 1993]. Each day of processing then results in two solution files (one global and one regional) with loosely constrained estimates of station coordinate, satellite orbit and Earth orientation parameters, and their corresponding covariance matrices.

Generation of Raw Time Series

The global and regional GAMIT solution files (two per day) are input as pseudo-observations to the GLOBK software [*Herring*, 1995] to estimate a consistent and continuous time series of daily three-dimensional positions for each PGGA site. Deterministic and stochastic parameters are estimated sequentially by a Kalman filter [*Herring et al.*, 1990]. The deterministic parameters include station coordinates and velocities for all global (non-PGGA) sites. The coordinates and velocities of a subset of global stations are tightly constrained and define the reference frame as described below. The stochastic parameters are very loosely constrained (between successive days) and include the PGGA site coordinates, satellite orbit, and Earth orientation (polar motion and UT1 rate) parameters. The estimation algorithm includes a forward filter and a smoothing filter. The smoothing filter involves running the forward filter with time in reverse and then taking the weighted mean of the forward and backward runs [*Herring et al.*, 1990].

Reference Frame

During the Landers earthquake, all PGGA sites experienced coseismic displacements, demonstrating the difficulty of maintaining a geodetic reference frame within the zone of deformation. The IGS provided, for the first time, a global terrestrial reference frame for GPS analysis with respect to which absolute station coordinates could be estimated. This reference frame is realized by the time-tagged coordinates and velocities of 13 "core" global tracking stations (Figure 2) with respect to the International Terrestrial Reference Frame 93 (ITRF93) maintained by the International Earth Rotation

Table 3. GPS Data Processing Differences Between Operational PGGA Analysis and This Analysis

Category	Original Analysis	This Analysis	Significance
Terrestrial reference frame	ITRF91	ITRF93	improved site coordinate and orbital parameter estimation
Type of analysis	one simultaneous solution of global and regional site data	distributed: one global and one regional solution	more efficient
Data editing	significant interactive editing	new automatic data editor, minimal interactive editing	improved efficiency and reliability, less subjective
Sampling rate	120 s	120 s global, 30 s regional	improved automatic data editing for regional solutions
Antenna phase center models	L1 and L2 constant vertical offsets only	yes for Rogue and Trimble antennas, no for Ashtech	better absolute vertical coordinates
Atmospheric model	latitude-dependent error in calculating satellite elevation angle	correct calculation of satellite elevation angle	approximately 10 parts per billion improvement in site coordinates
Atmospheric parameters	1 zenith delay per site	1 zenith delay every 2 hours, piecewise continuous	better accuracy in vertical component
Ambiguity resolution	none	in regional solution	better accuracy in east component

Analyses are performed with the GAMIT software [*King and Bock*, 1995].

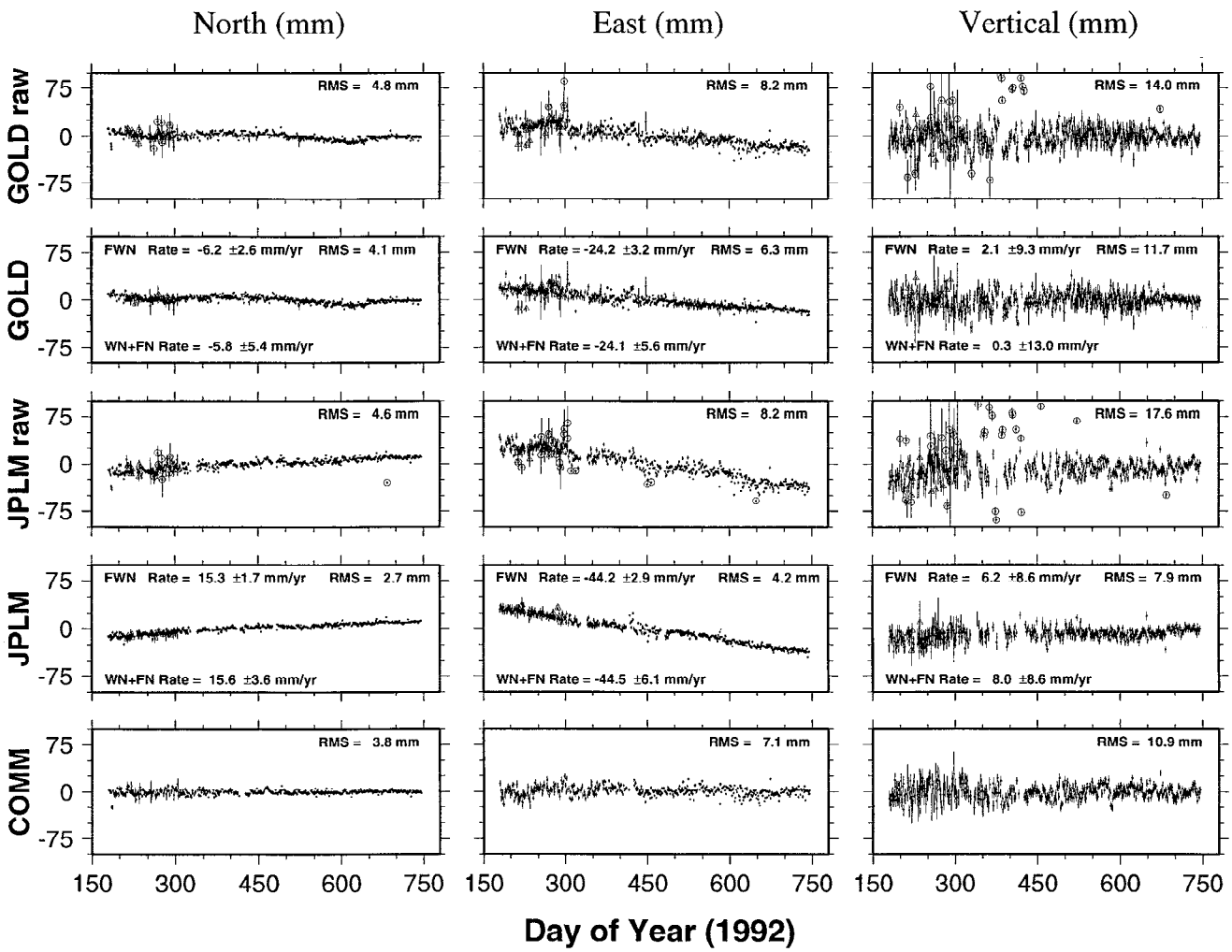

Figure 5. Demeaned raw and filtered position time series for north, east, and vertical components of sites GOLD and JPLM. The circled points in the raw time series are considered outliers and are deleted from further analysis. The triangulated points indicate days when GPS anti-spoofing (AS) was active. Listed for each filtered time series is the rate computed by linear regression and its uncertainty (95% confidence interval), under the fractal white noise (FWN) model and the white noise plus flicker noise (WN+FN) model [*Zhang et al.*, this issue], and the weighted RMS scatter of the detrended time series. The bottom panel shows the common-mode bias removed daily from the raw time series (cleaned of outliers) of each site to construct the filtered time series.

Service [*Boucher et al.*, 1994]. Since GOLD, a core IGS station, is located in a region of active deformation (the Mojave shear zone) we do not constrain its coordinates but rather the coordinates of DRAO (Penticton, British Columbia.). During the period between the Landers and Northridge earthquakes, DRAO was the closest IGS site outside of southern California, more than 3000 km to the north (Figure 2).

Zhang [1996] demonstrated that there exist strong statistical correlations among absolute coordinate estimates of regional networks and weak correlations between the coordinate estimates of regional and global networks. Any global errors are expected to propagate in a similar manner to all regional site estimates, in particular, satellite orbit, Earth orientation, and reference frame errors. A comparison of the raw position time series for all PGGA sites reveals that there is indeed a systematic bias in each coordinate component which is distinguishable from site-specific effects [*Wdowinski et al.*, this issue]. Considering the large spatial extent of the PGGA network, we attribute these biases entirely to global errors and rule out any tectonic origin (see bottom panel of Figure 5 for a plot of common-mode signal over time). The relatively large scatter in the raw positions is due to the great distance to the nearest IGS site, since reference frame errors are known to increase with distance from the nearest fiducial station [e.g., *Bock*, 1982].

Spatial Filtering

Wdowinski et al. [this issue] present an algorithm to filter out the common-mode spatial bias from the raw site positions in order to increase their signal-to-noise ratio for estimating coseismic and postseismic site displacements. Detrended time series from all stations are summed and averaged to compute the common-mode bias for each station coordinate. Individual baseline components are unaffected since the same numerical value is subtracted from all time series. Site velocities are also unchanged. This approach allows for a more effective

estimation of the GPS error spectrum and hence separation of geodetic "noise" and geophysical "signal," on a site-by-site basis.

Coordinate Time Series Between Landers and Northridge Earthquakes

Seven sites (GOLD, JPLM, PIN1, PIN2, ROCH, SIO3, VNDP) have observations spanning the entire period between the 1992 Landers and 1994 Northridge earthquakes (Figure 1). All experienced coseismic displacements during the Landers earthquake; the latter three (PIN1, PIN2, ROCH) also underwent short-term postseismic displacements [*Wdowinski et al.*, this issue]. Two sites (JPLM and PVEP) experienced observable coseismic displacements during the Northridge earthquake [*Bock*, 1994; *Hudnut et al.*, 1996]. Three sites (HARV, MATH, PVEP) became operational less than a year before the Northridge earthquake.

Data Cleaning and Filtering

Ideally, the same equipment and procedures should be used over the lifetime of a project to ensure that the statistics of the coordinate time series are uniform. In practice, this is difficult to achieve and may be undesirable in some cases if the benefits of incorporating improvements in GPS hardware and firmware outweigh the costs of creating a heterogeneous data set. Only sites GOLD and JPLM (operated by the group at the Jet Propulsion Laboratory) have nearly complete continuous series with little data loss and no changes of hardware for the entire period between the two earthquakes. Because of hardware failures, lack of spare parts, and budgetary restrictions, we were forced to make several instrument changes at the PIN1 and VNDP sites, between Rogue and Ashtech GPS systems, which impacted the position time series. The most serious effects were due to antenna changes from Rogue Dorne-Margolin antennas with choke rings to Ashtech P1/P2 Rev B antennas which have poorly modeled antenna phase center characteristics [*Schupler et al.*, 1994]. The antenna switches caused discontinuities of order 100 mm in the vertical component but also significant horizontal discontinuities as described below. Hardware, communication, and operator failures caused some gaps in the time series at several sites. Sites SIO3, VNDP, PIN1, PIN2, and ROCH have two significant data gaps each. Incomplete 24-hour data sets resulted in either larger error bars and/or outliers during a small number of observing days at several sites. Erratic observations due to hardware failures for the first 120 days of data collected affected sites PIN1, PIN2, and ROCH; PIN1 also suffered from repeated AS tests conducted in the early part of the observing period and three discontinuities in its time series due to instrument changes. Time series analysis of the PGGA data between the Landers and Northridge earthquakes was complicated by these problems.

We tailored the basic algorithm described by *Wdowinski et al.* [this issue] to stack the raw PGGA time series and filter out a common-mode regional bias. The steps taken include the following:

1. Detrending. Removing a linear trend from the time series. When an antenna jump is expected (see step 2), detrending is performed separately for data before and after the jump.

2. Antenna offset correction. Correcting discontinuities due to antenna changes. The offsets at PIN1 and VNDP needed to be corrected so that they would not bias the other series in the stacking procedure (step 4). The magnitudes of the discontinuities were estimated by averaging the detrended positions for a few weeks before and after the discontinuity and differencing the positions (Table 4a). The filtered series provided more sensitivity to correcting the discontinuities than the cleaned series (see step 6).

3. Outlier Detection. Cleaning the series of data outliers. For PIN1 and VNDP, outliers were identified within each continuous subset of data, using simple rejection criteria described by *Wdowinski et al.* [this issue].

4. Stacking. Summing and averaging the cleaned series to determine a common-mode bias. The GOLD and PVEP data were excluded from the stacking because of apparent fluctuations in their time series (Figure 5) attributed to monument and/or site instability. Data from PIN1, PIN2, and ROCH were excluded for the 120-day period from June 28 to October 26, 1992, since these data were sparse (due to equipment failures and operator errors), unusually erratic (at PIN1 due to GPS AS), and affected by short-term postseismic displacements [*Wdowinski et al.*, this issue].

5. Filtering. Removing the common-mode bias from the cleaned series. The bias was subtracted from all series, including the data from sites that were not used in the stacking.

6. Antenna offset correction. Correcting discontinuities due to antenna changes. Same procedure as step 2, but using the filtered series. Filtering of the time series for PIN1 indicated that the receiver/antenna switches also caused small but significant discontinuities in the horizontal component time series (Table 4a). It proved difficult to estimate the remaining PIN1 offsets solely from the filtered series. For example, repairing the discontinuity of September 25, 1992, was complicated by the postseismic signal at Piñon Flat Observatory [*Wdowinski et al.* this issue], and the large data gap thereafter resulting from hardware failure (Table 4a shows the large uncertainty in the offset estimated

Table 4a. Record of Estimated Vertical and Horizontal Coordinate Offsets at PIN1

Site	Change	Date of Change	Vertical, m	North, m	East, m
PIN1	Rogue to Ashtech	Sept. 25, 1992	0.110 ± 0.010	—	—
PIN1	Ashtech to Rogue	June 24, 1993	-0.114 ± 0.002	-0.0046 ± 0.001	0.0043 ± 0.001
PIN1	Rogue to Ashtech	Nov. 6, 1993	0.092 ± 0.002	0.0019 ± 0.001	-0.0051 ± 0.001
VNDP	Ashtech to Rogue	Jan. 12, 1993	-0.106 ± 0.003	—	—

Vertical offsets are estimated from the raw time series to compensate for changes of GPS receiver/antenna. (Refer to Table 1.) Horizontal offsets are estimated from the filtered time series. Residual vertical offsets are not detectable in the filtered time series. Uncertainties are 1σ values.

Table 4b. Velocity Comparison Before and After Correction for PIN1 Offsets

Component	PIN1 (Before), mm/yr	PIN1 (After), mm/yr	PIN2, mm/yr
North	8.7 ± 0.3	11.9 ± 0.3	12.2 ± 0.3
East	-29.8 ± 0.7	-28.5 ± 0.6	-28.9 ± 0.6
Vertical	3.7 ± 1.3	7.0 ± 1.4	4.5 ± 1.3

PIN1 experienced 3 hardware changes, recorded in Table 4a. PIN2 velocity is shown for comparison since it experienced no hardware changes. Uncertainties are 1σ values.

for the September 25, 1992, discontinuity). To correct the PIN1 series for these small horizontal offsets, we took advantage of the continuous time series for site PIN2, only 50 m away. With the knowledge that both sites have well-anchored stable monuments, we assumed that any abrupt offsets between the PIN1-PIN2 (baseline) time series were due entirely to the PIN1 discontinuities (this assumption does nothing to align the velocities of PIN1 and PIN2). We give the formal rate estimates of the PIN1 site both before and after the final offset corrections in Table 4b and also list the estimated PIN2 rate for comparison. There is a large difference between the rate estimates before and after the offset corrections, especially in the north (3.2 mm/yr) and vertical (3.3 mm/yr) components. We see that after correcting for the offsets in the PIN1 time series, the velocities agree more closely (again, we have done nothing to constrain the velocities to be the same).

Steps 1–6 were iterated until there were no more detected outliers and residual offset estimates were less than 1 mm.

Final Time Series

The final filtered daily coordinate time series in north, east, and vertical components are shown in Figures 5 and 6 for the 10 PGGA sites for the 19-month period between the Landers and Northridge earthquakes. The raw and filtered coordinate time series for sites JPLM and GOLD are compared in the top four panels of Figure 5. The bottom panel shows the common-mode regional signal as a function of time. The filtered time series for the remaining sites are shown in Figure 6. Henceforth "the time series" refers to the filtered time series.

Site Velocity Estimation

Zhang et al. [this issue] investigate four noise models for the PGGA time series. The first three are a white noise model, a white noise plus flicker noise model, and a white noise plus random walk noise model. In the frequency domain, the spectral index of white noise is zero (a flat spectrum), the spectral index of flicker (1/f) noise is one, and the spectral index of random walk ($1/f^2$) noise is two. Of these three models, the white noise plus flicker noise model best fits our data. This analysis is performed in the time domain using a maximum likelihood estimation (MLE) algorithm [*Langbein and Johnson*, 1997] which is limited to noise models with integer-valued spectral indices. *Zhang et al.* [1997] also investigate in the frequency domain a fourth model which assumes that the noise can be described by a single-parameter power law process. They find that a fractal white noise model with a spectral index of about 0.4 also fits the PGGA time series. In the following, PGGA site velocity uncertainties have been estimated using both the white noise plus flicker noise model and the fractal white noise model (see rate estimates in Figures 5 and 6). If longer time series than these show the noise spectrum to be more colored (i.e., higher spectral index at the low frequencies) than indicated by these models, then the velocity uncertainties will have to be increased appropriately.

Discussion of PGGA Site Velocities

The PGGA recorded the June 28, 1992 (M_W=7.3), Landers earthquake, the largest magnitude earthquake in California in the past 40 years. Nineteen months later, it recorded the January 17, 1994 (M_W=6.7), Northridge earthquake, the strongest earthquake to strike the Los Angeles basin in two decades. We discuss whether PGGA site velocities estimated by *Zhang et al.* [this issue] for the period between these two earthquakes (Figure 7) have changed in comparison with the velocities estimated by *Feigl et al.* [1993] from 5–10 years of VLBI and GPS measurements prior to the Landers earthquake.

Wdowinski et al. [this issue] estimate, for each PGGA site, coseismic displacements induced by the Landers earthquake. In addition, they find postseismic deformation at Piñon Flat Observatory of magnitude 6±2 mm (15% of the coseismic displacement) modeled as short-term (22±10 days) postseismic exponential relaxation superimposed upon a long-term linear displacement rate. Postseismic horizontal displacements of longer duration estimated primarily from GPS field survey data were reported by *Shen et al.* [1994] with a decay time of about 38 days. *Savage and Svarc* [1997] estimated a decay time of 84±23 days superimposed upon a longer linear trend, based on data from a linear array of GPS monuments across the Emerson fault segment of the Landers rupture. They attributed the linear trend to a slower postseismic relaxation with a decay time greater than 5 years. INSAR-determined postseismic displacements result in a significantly longer relaxation time, 270±45 days estimated by *Peltzer et al.* [1996] but only in a very limited region adjacent to the fault. In contrast to the studies of *Peltzer et al.* [1996] and *Savage and Svarc* [1997], however, our observations are taken in the far field, 65 km (PIN1/PIN2) to 300 km (VNDP) from the Landers rupture zone. Other than the short-term postseismic deformation at the Piñon Flat Observatory reported by *Wdowinski et al.* [this issue] we cannot distinguish in the 19-month PGGA time series any tectonic signal besides a linear trend, with no apparent decay in the velocity of the sites.

Site velocities estimated by *Feigl et al.* [1993] in central and southern California between 1984 and 1992 provide interseismic displacement rates at a number of PGGA site locations prior to the Landers earthquake. Five sites, JPLM, PIN1/2, PVEP, SIO3, and VNDP (Figure 1), are within 2 km of sites described by *Feigl et al.* [1993], and one site, GOLD, is 10 km away, giving us the opportunity to compare pre- and

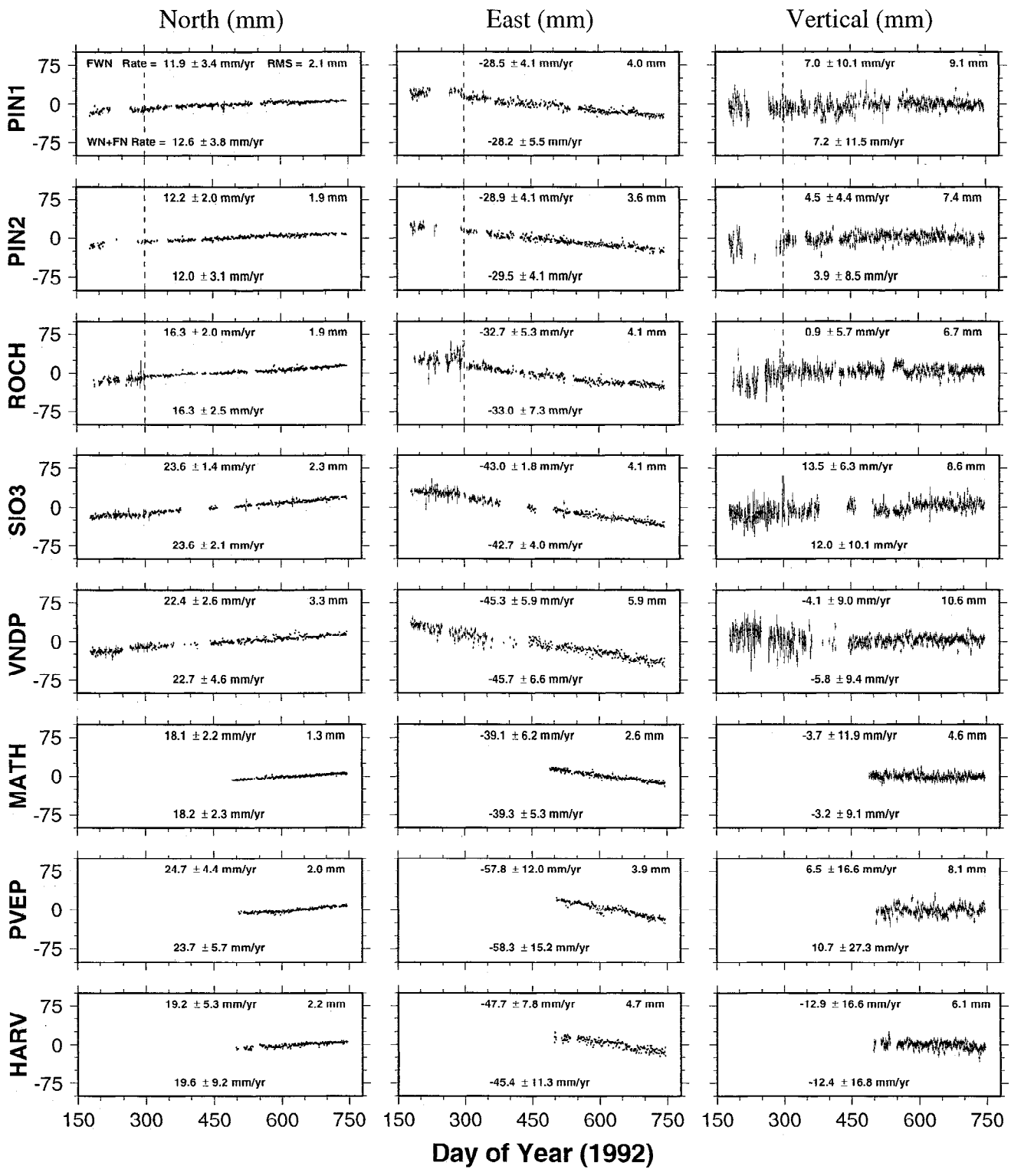

Figure 6. Demeaned filtered position time series for north, east, and vertical components of the PGGA sites (GOLD and JPLM shown in Figure 5). Listed above each time series is the rate computed by linear regression and its uncertainty (95% confidence interval), under the fractal white noise (FWN) model and the white noise plus flicker noise (WN+FN) model [*Zhang et al.*, this issue], and the weighted RMS scatter of the detrended time series. The rate for the vertical component of ROCH was not estimable under the WN+FN model. All data to the left of the vertical dashed lines for sites PIN1, PIN2, and ROCH have been omitted from the time series analysis as described in the text.

post-Landers crustal velocities at these locations (Table 5). These two data sets, however, are not without problems. Two of the sites (SOLJ near SIO3, analyzed by *Feigl et al.* [1993] and PVEP, analyzed by us) are ignored in this comparison since they have a limited number of measurements. Furthermore, two sites analyzed by *Feigl et al.* [1993] have shorter VLBI observation spans (4 years for JPL1 and 6 years for PINY) and sparser GPS and VLBI data than available for

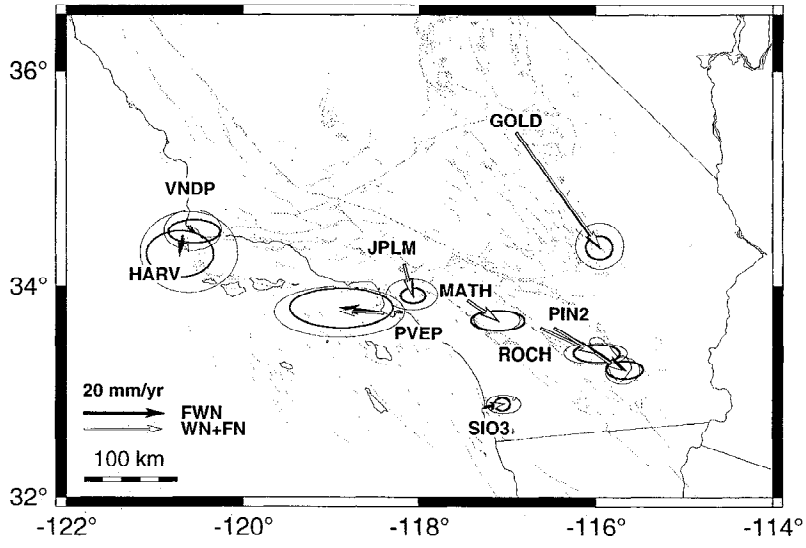

Figure 7. Observed horizontal site velocities (millimeters per year) relative to the NUVEL-1A Pacific plate. The velocities and their uncertainties are estimated from the PGGA time series (Figures 5-6) by linear regression, under the fractal white noise (FWN) model and the white noise plus flicker noise (WN+FN) model [*Zhang et al.*, this issue]. Estimates of north and east components are assumed to be uncorrelated. Uncertainties are displayed as 95% confidence ellipses.

sites MOJA and VNDN and hence have larger velocity uncertainties (Table 5). Finally, PGGA data collected at Piñon Flat Observatory have been omitted for the 3-month period immediately following the Landers earthquake because of a combination of large gaps, unusually larger day-to-day scatter, and the presence of short-term postseismic deformation [*Wdowinski et al.*, this issue] which would bias the velocity estimates. We compare the PGGA results for site PIN2 because of the complications due to hardware changes at PIN1 as discussed earlier (this has no impact, though, on our subsequent conclusions).

Feigl et al. [1993] presented site velocities relative to the NUVEL-1A Pacific plate [*DeMets et al.*, 1990, 1994], a frame that they realized by applying rotation and translation rates to their velocities to minimize the measured horizontal velocities at 10 sites on the North American plate. The transformation from this North America fixed frame to a Pacific plate frame was achieved using the NUVEL-1A relative motion Euler vector. PGGA velocities are computed in the global ITRF93 reference frame, which has small rotation rates [*Boucher et al.*, 1994] with respect to the no-net-rotation (NNR) NUVEL-1A plate motion model [*Argus and Gordon*, 1991]. To align the PGGA velocity vectors computed by *Zhang et al.* [this issue] with those of *Feigl et al.* [1993], we rotate the former, first into NNR NUVEL-1A and then into a fixed (NUVEL-1A) Pacific plate frame. The pre- and post-Landers velocities are displayed in Figure 8 (and recorded in Table 5) for sites GOLD, JPLM, PIN2, and VNDP. The 10-year VLBI/GPS and 19-month PGGA velocities for VNDP (expected to be close to Pacific plate velocity) agree within 1–2 mm/yr, and their differences are not statistically distinguishable from zero. The agreement between the VNDP and VNDN velocities gives us confidence that the two reference frames are closely aligned. VNDP experienced little Landers-induced coseismic deformation [*Wdowinski et al.*, this issue], and as expected, we see no significant change in the post-Landers velocity. Rather than make the comparisons with respect to the Pacific plate we could assume zero-velocity for VNDP (thus minimizing any errors due to the plate motion model) and compute the relative velocities of the other three sites with respect to VNDP. Doing this increases slightly the statistical significance of the ensuing velocity differences at the other

Table 5. Horizontal Site Velocity Estimates Before and After the Landers Earthquake

Site Code (This Study)	Site Code [*Feigl et al.*, 1993]	Component	Post-Landers FWN Model	Post-Landers WN+FN Model	Pre-Landers [*Feigl et al.*, 1993]
GOLD	MOJA	North	-29.1 ± 2.6	-28.6 ± 5.4	-26.6 ± 0.6
		East	21.1 ± 3.2	21.2 ± 5.6	23.9 ± 0.6
JPLM	JPL1	North	-7.8 ± 1.7	-7.5 ± 3.6	-11.5 ± 1.8
		East	2.3 ± 2.9	2.1 ± 6.1	2.7 ± 2.2
PIN2	PINY	North	-10.8 ± 3.4	-10.1 ± 3.8	-13.2 ± 1.8
		East	18.2 ± 4.2	18.5 ± 4.5	13.3 ± 2.0
VNDP	VNDN	North	-1.3 ± 2.5	-1.0 ± 4.7	-1.0 ± 0.8
		East	1.5 ± 5.9	1.1 ± 6.6	0.3 ± 0.8

Post-Landers velocities are estimated by *Zhang et al.* [this issue] for the fractal white noise (FWN) and white noise plus flicker noise (WN+FN) models. Velocities have units of millimeters per year and are with respect to the NUVEL-1A Pacific plate. Velocity uncertainties are 95% confidence intervals. See also Figure 8. Pre-Landers uncertainties include a factor applied by *Feigl et al* [1993] to the formal errors to account for long-term repeatability.

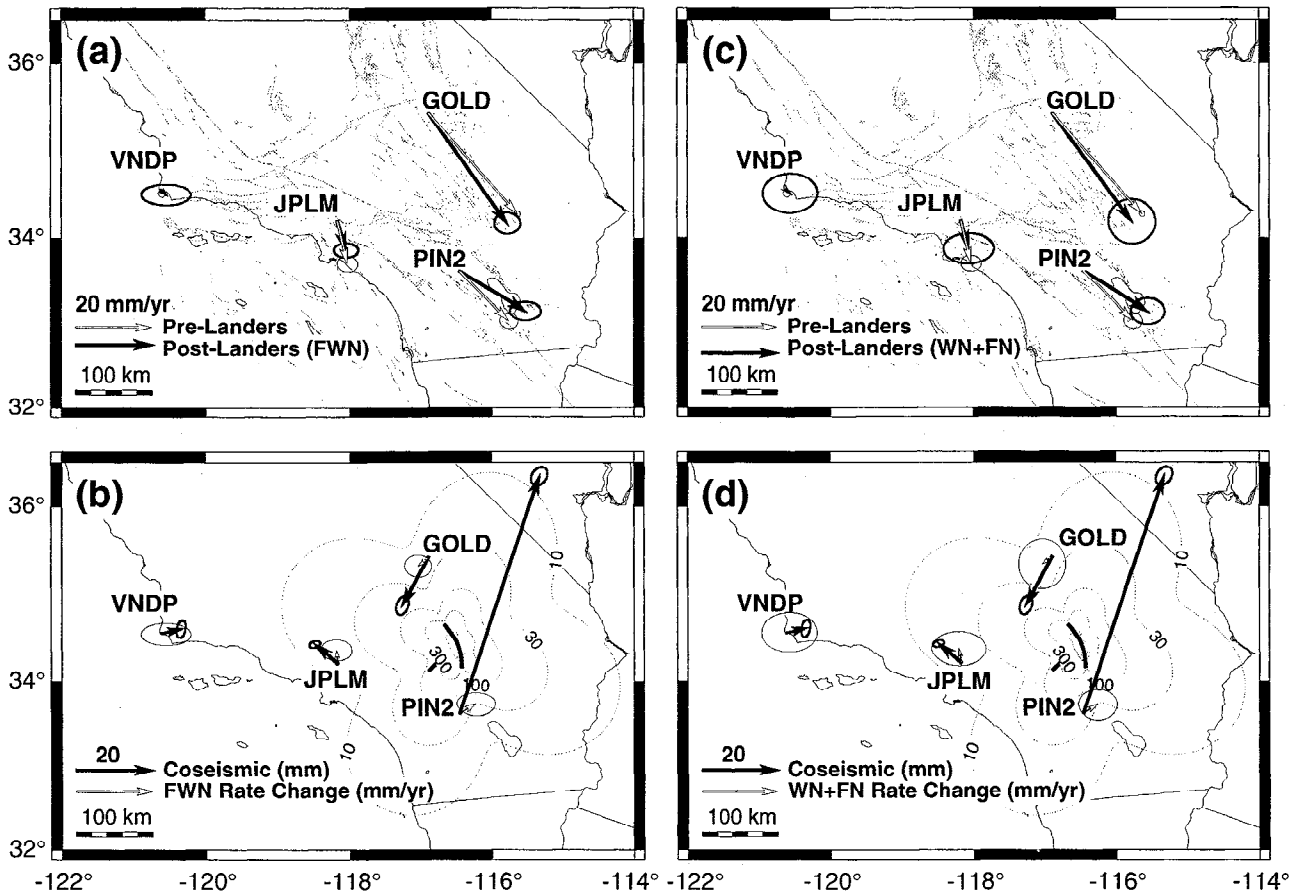

Figure 8. Change in regional deformation rates induced by the 1992 Landers earthquake. All ellipses are 95% confidence. (a) and (c) Pre-Landers site velocities estimated by *Feigl et al.* [1993] and post-Landers PGGA velocities estimated by *Zhang et al.* [this issue], for the fractal white noise (FWN) and white noise plus flicker noise (WN+FN) models. Velocities are in units of millimeters per year and are with respect to the NUVEL-1A Pacific plate. (b) and (d) PGGA observed coseismic displacements induced by the Landers earthquake, the trace of the earthquake's surface rupture (arc segment), the Big Bear earthquake's subsurface trace (line segment), and model coseismic contours are adapted from *Wdowinski et al.* [this issue]. Observed and contoured model coseismic displacements are in units of millimeters. Post-Landers velocity changes are the result of differencing the post-Landers velocities from the pre-Landers velocities, for the FWN and WN+FN models.

sites, 65–100 km from the Landers earthquake epicenter. However, we choose to present our results with respect to the fixed Pacific plate because not constraining the motion at VNDP provides an important additional observation on the far-field (300 km) displacements.

The pre- and post-Landers velocity estimates with respect to the Pacific plate indicate shortening of the velocity vector at JPLM but no change in direction, clockwise rotation of the GOLD vector, and anticlockwise rotation of PIN2 but no significant change in magnitude at either site. Furthermore, a comparison of the pre- and post-Landers horizontal velocities indicates that the directions of the three velocity vector differences are strongly coupled with the corresponding directions of coseismic surface slip (Figures 8b and 8d). These velocity changes cannot be attributed to a simple reference frame misalignment, for example, a horizontal rotation, and the directions of coseismic displacements are only weakly dependent on the chosen reference frame.

The confidence level assigned to the velocity change uncertainties is crucial considering the small magnitude of the estimated changes (3–5 mm/yr) and the potential importance of these findings. The time series analysis of *Zhang et al.* [this issue] indicates, as described earlier, that a white noise model is inappropriate for the 19-month PGGA data and that either a white noise plus flicker noise model or a fractal white noise model with a spectral index of about 0.4 best fit the data. In short, the procedure for either of the PGGA noise models includes estimating three parameters for each component time series including the velocity, and either the spectral index and scale factor (power level) for the fractal white noise process, or the scaling coefficients for both a white and a flicker noise process, as well as the corresponding (three-dimensional) standard error ellipsoid. Estimating the vector velocity uncertainty introduces an additional degree of freedom (for a total of four) when assigning (95%) probabilities to the corresponding confidence region. To compare the pre- and post-Landers velocity vectors, we first project the four-dimensional PGGA confidence regions into the two-dimensional vector velocity plane. We ignore correlations between the north and east velocity components since a preliminary network adjustment of the GPS positions indicates that these correlations are of magnitude 0.1 or smaller and are therefore negligible.

Feigl et al. [1993] reported velocity uncertainties derived from scaling the formal uncertainties by a single factor based approximately on the long-term repeatabilities of the baseline

components and the chi-square per degree of freedom for the combined GPS and VLBI solution. They acknowledged correlations in the measurements but did not attempt to determine the form and parameters of a noise model specific to individual stations or baseline components. Of the components being compared with the PGGA times series, all but the north velocities of JPLM and PINY are dominated by the VLBI data (see Figure A6 of Feigl et al.) We analyzed the VLBI time series using the methods applied to the PGGA series and found that uncertainties estimated by Feigl et al. are realistic or conservative for most components, but may be too small by as much as 50% for the east velocity of MOJA. The GPS data used for JPLM and PINY are a combination of PGGA observations (May 1991 - October 1992) and four 4- to 5-day surveys, together spanning less than 3 years. The small number of samples (compared to other stations in the Feigl et al. network) gives us less confidence in the GPS uncertainties for these two stations. On the other hand, the 95% confidence ellipses for the VLBI-only, GPS-only, and combined solutions for JPLM and PINY easily overlap, a check used by Feigl et al. to validate the scaling of their uncertainties.

We computed the uncertainties in the velocity differences using standard propagation of errors, also assuming that the post-Landers PGGA and pre-Landers *Feigl et al.* [1993] estimated site velocities are uncorrelated (i.e., we simply add the corresponding two-dimensional covariance matrices). We show in Figure 9 the 95% confidence regions for the pre- and post-Landers velocity vectors and their vector differences, under both the fractal white noise and white noise plus flicker noise models. Under the fractal white noise model we find that the preearthquake and postearthquake velocities are statistically different at three sites (PIN2, GOLD, JPLM) located within 65–100 km of the Landers epicenter, at a significance level of 99%, for all three sites. The white noise plus flicker noise model results in corresponding significance levels of only 94%, 43%, and 88%. At site VNDP (about 300 km from the Landers rupture zone) the velocity differences are, as expected, statistically different from zero only at a negligibly low confidence level (0% and 2% significance level for the fractal white noise model and white noise plus flicker noise model, respectively).

Despite the limited number of sites available for this comparison, we believe that the observed post-Landers changes in site velocity from data recorded in the 19-month period after the earthquake are significant and are an indication of a regional (at least 100 km radius) change in displacement rates after a major earthquake. We acknowledge that the level of significance of these observations is dependent on the assumed noise model for the PGGA data and the limitations in assessing the uncertainties in the *Feigl et al.* [1993] data as described above. However, our conclusion of a real tectonic signal is not only based on the results of the statistical analysis but also on the observation that the velocity changes are strongly coupled with the direction of coseismic surface deformation at GOLD, JPLM, and PIN2 (not so for the more distant site VNDP). The conventional explanation for the velocity differences is that our results indicate a longer time constant of postseismic relaxation than has been observed previously. That is, if we assume that the change in rate has a typical exponential decay with time, we can estimate that the relaxation time must be greater than 800 days, which is also longer than the length of our time series. Alternatively, it is conceivable (but unlikely) that the steady state velocity field actually changed and will prove to be time-intransient, at least until a future major earthquake produces another such effect.

There are a variety of possible causes for the postseismic rate changes. The PGGA observations are consistent with fault-normal shortening that is superimposed on right-lateral slip at depth along the Landers fault trace. Our reference line for the continuation of the fault trace is the indentation of contours of the coseismic displacement (Figures 8b and 8d). *Savage and Svarc* [1997] observe fault-parallel GPS site displacements that are consistent with right-lateral slip on the downward extension of the rupture trace, and fault normal

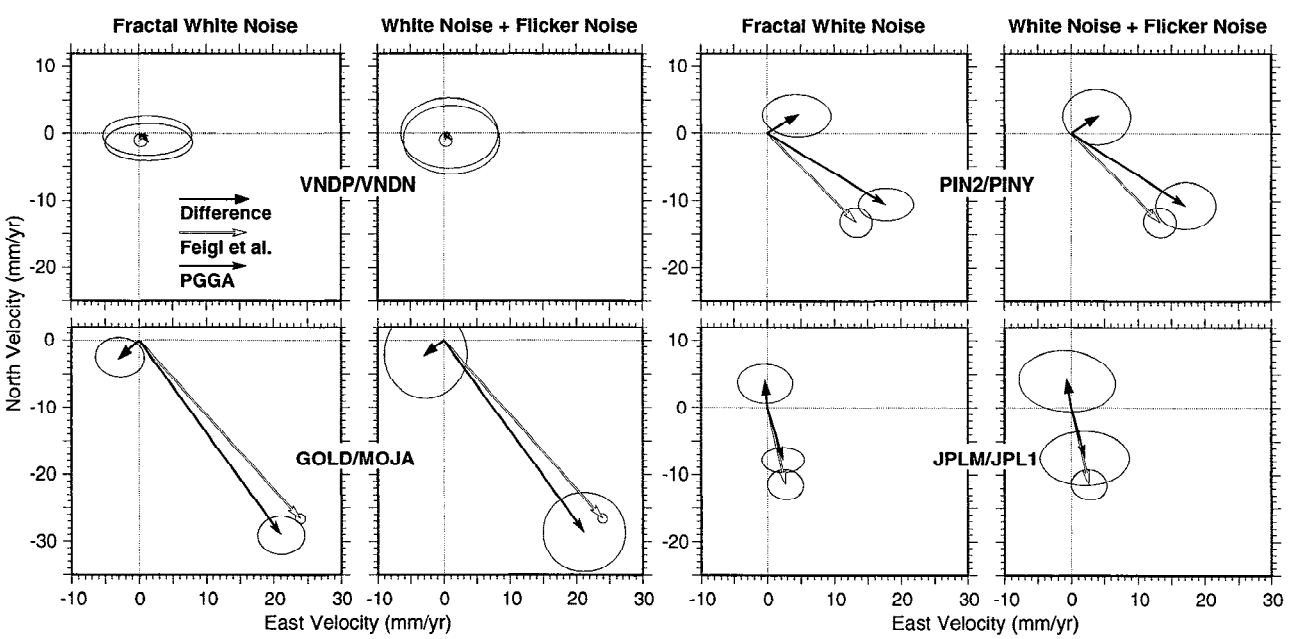

Figure 9. Site-by-site 95% confidence regions for the pre-Landers velocity vectors [*Feigl et al.*, 1993], post-Landers velocity vectors [*Zhang et al.*, this issue], and velocity differences under the fractal white noise and the white noise plus flicker noise models for the PGGA time series. Velocities are in units of millimeters per year and are with respect to the NUVEL-1A Pacific plate.

displacements (collapse along one segment of the fault and extension along another segment) which they attribute to the curvature of the rupture. *Massonnet et al.* [1996b] also describe their INSAR results in terms of fault-parallel and fault-normal components. The fault-parallel component indicates right-lateral displacement while the fault-normal component indicates shortening or postseismic collapse, which they attribute to crack closure and fluid expulsion mechanisms. *Peltzer et al.* [1996] attribute INSAR-observed postseismic collapse to a transition in the Poisson's ratio of the deformed volume of rock caused by pore fluid flow. Other possible causes for the observed PGGA postearthquake rate changes (in particular at such large distances from the Landers rupture zone) are related to viscous relaxation at depth [e.g., *Thatcher*, 1983; *Li and Rice*, 1987; *Lyzenga et al.*, 1991; *Ben-Zion et al.*, 1993; *Reches et al.*, 1994; *Ivins*, 1996, *Ivins and Sammis*, 1996].

The notion that crustal deformation displays transient stages that include large spatial variations in velocities over deformation zones with a radius as wide as 100 km (the distance of site JPLM from the Landers rupture zone) but less than 300 km (the distance of site VNDP) is intriguing. These long-wavelength signals, if they do indeed exist, could provide critical data for a better understanding of earthquake and crustal deformation processes. Analysis of considerably longer spans of PGGA data, as well as reanalysis of the pre-Landers VLBI and GPS data with improved models, will provide additional insight into the nature of the observed deformation.

Conclusions

We have developed a system to sample the crustal deformation cycle based on data collected by an array of continuously monitoring GPS sites in southern California. Coordinates of each site are estimated daily for the 19-month time interval between the 1992 Landers and 1994 Northridge earthquakes with respect to a global reference frame defined by the positions and velocities of global GPS tracking stations, all external to this diffuse plate boundary.

We compare at four site locations displacement rates estimated in the companion paper by *Zhang et al.* [this issue] with those reported by *Feigl et al.* [1993], which were derived from an independent set of GPS and VLBI measurements collected over nearly a decade prior to the Landers earthquake. We find changes in displacement rates after the Landers earthquake at three sites 65–100 km from the epicenter. The velocity differences range between 3 and 5 mm/yr in magnitude and are systematically coupled to the directions of the corresponding coseismic displacements. Velocities at the fourth site 300 km from the epicenter show no significant changes in displacement rate.

The comparison between these two sets of displacement rates is complicated by our incomplete knowledge of the noise properties of the two time series. Additional analysis of the preearthquake data and of longer PGGA time series will better quantify the nature of regional postseismic deformation after the Landers earthquake and will be addressed in future work. In particular, there exist more data (both VLBI and GPS) from the pre-Landers period than were analyzed by *Feigl et al.* [1993]. Including these measurements should allow a more detailed investigation of noise properties of the pre-Landers data in a manner similar to that employed in *Zhang et al.* [this issue] for the PGGA data.

The detection of long-wavelength signals induced by the Landers earthquake points out the importance of distributing continuous GPS stations across the entire width of the diffuse plate boundary in southern California. Our observations are limited by the small number of continuous GPS sites operating here during this critical period, the presence of colored noise in the data, and the relatively short time interval between the two earthquakes. It is clear that continuous data from a denser array need to be collected over longer periods of time in order to better sample crustal deformation in time and space. Longer time series will also improve our understanding of the error spectrum of GPS measurements of site position. However, continuous and homogeneous time series in the southern California milieu are often interrupted by significant seismic events so that simultaneous improvements in our understanding of crustal deformation and the GPS error spectrum may only be obtained incrementally.

Acknowledgments. We thank Jim Savage for his encouragement (and patience) and providing post-Landers model displacements for sites at Goldstone and Piñon Flat Observatory. Suggestions by Mike Bevis and Brad Hager and reviews by Jeff Freymueller, Jim Savage, and Clark Wilson contributed to a much improved manuscript. The PGGA was established in 1990 by Scripps Institution of Oceanography and the Jet Propulsion Laboratory, with the participation of Massachusetts Institute of Technology, California Institute of Technology, University of California Los Angeles, U.S. Geological Survey (Pasadena), Riverside Flood Control and Water Conservation District, and Riverside County Transportation Division. We appreciate the support of our colleagues including Shelley Marquez, Myra Medina, Rosa Felice, Rosemary Leigh, Veronica Dubrovskaya, Paul Tregoning, Paul Henkart, Seiichi Shimada, Peter Worcester, Kevin Hardy, Steve Bralla, and Harold Bolton at Scripps Institution of Oceanography; John Scheid, Ulf Lindqwister, Mike Watkins, Bill Melbourne, Larry Young, Tim Dixon, Geoff Blewitt, Tom Yunck, Ruth Neilan, Tom Meehan, and the Deep Space Network group at JPL; Brad Hager and Simon McClusky at MIT; Gerald Doyle and Mark Madeiros at Riverside Flood Control and Water Conservation District; Gerald Stayner and Brian Hess at the Riverside Transportation Division; Don Hunter, John Fundus, and Larry Fenske at Caltrans; Steve Salyards and Zheng-kang Shen at UCLA; Hiroo Kanamori, Egill Hauksson, and Kerry Sieh at Caltech; Jonathan Ladd, Tom Hunter, Sergei Gourevitch, and James Stowell at Ashtech, Inc.; Ken Moymann at Trimble Navigation; and Boudewijn Ambrosius at Delft University of Technology. We thank John Orcutt, Bernard Minster, Edward Frieman, and Tom Collins at Scripps for their encouragement and support of this work since its inception, and Kei Aki, Tom Henyey, and John McRaney at SCEC/USC. Our many colleagues at the International GPS Service for Geodynamics and the International Earth Rotation Service have graciously made the global tracking and reference frame data available. The first author thanks the Department of Civil Engineering at Technion, Israel Institute of Technology, and the Department of Geophysics and Planetary Sciences at Tel Aviv University for providing resources and a comfortable working environment during his two extended stays in Israel. The maps and figures were generated using the Generic Mapping Tools (GMT) software version 3 released in August 1995 [*Wessel and Smith*, 1991]. This work was supported by NASA (NAGW-2641, NAG-5-1917, NASW 3007, NAG5-3550), USGS (14-08-0001-G1673, 1434-92-G2196, 1434-95-G2629), NSF (EAR 92 08447, EAR 94 16338), SCEC (PO 569930, Cooperative Agreement EAR-8920136, USGS Cooperative Agreement 14-08-001-A0899), Riverside County Flood and Water Conservation District, Riverside County Transportation Division, and California Department of Transportation. Part of the second author's salary was provided by the Ida and Cecil Green Fellowship. This is paper 328 of the Southern California Earthquake Center.

References

Argus, D. F., and R. G. Gordon, No-net-rotation model of current plate velocities incorporating plate rotation model NUVEL-1, *Geophys. Res. Lett.*, *18*, 2039-2042, 1991.

Bennett, R. A., R. E. Reilinger, W. Rodi, Y. Li, and M. N. Toksöz, Coseismic fault slip associated with the 1992 *M* 6.1 Joshua Tree,

California, earthquake: Implications for the Joshua Tree-Landers earthquake sequence, *J. Geophys. Res., 100*, 6443-6461, 1995.

Ben-Zion, Y., J. R. Rice, and R. Demowska, Interaction of the San Andreas fault creeping section with adjacent great rupture zones and earthquake recurrence at Parkfield, *J. Geophys. Res., 98*, 2135-2144, 1993.

Beutler, G., P. Morgan, and R. E. Neilan, International GPS Service for Geodynamics: Tracking satellites to monitor global change, *GPS World, 4 (2)*, 40-46, 1993.

Beutler, G., I. I. Mueller, and R. E. Neilan, The International GPS Service for Geodynamics (IGS): Development and start of official service on January 1, 1994, *Bull. Géod. 68*, 39-70, 1994.

Bevis, M., S. Businger, T. Herring, C. Rocken, R. Anthes, and R. Ware, GPS meteorology: Remote sensing of atmospheric water vapor using the Global Positioning System, *J. Geophys. Res., 97*, 15,787-15,801, 1992.

Bevis, M., Y. Bock, P. Fang, R. Reilinger, T. A. Herring, J. Stowell, and R. Smalley, Blending old and new approaches to regional GPS geodesy, *Eos Trans. AGU, 78*, 61, 1997.

Blewitt, G., Carrier phase ambiguity resolution for the Global Positioning System applied to geodetic baselines up to 2000 km, *J. Geophys. Res., 94*, 10,187-10, 283, 1989.

Blewitt, G., An automatic editing algorithm for GPS data, *Geophys. Res. Lett., 17*, 199-202, 1990.

Blewitt, G., Advances in Global Positioning System technology for geodynamics investigations: 1978-1992, in *Contributions of Space Geodesy to Geodynamics: Technology*, edited by D. E. Smith and D. L. Turcotte, pp. 195-213, *Geodyn. Ser.*, vol. 25, AGU, Washington, D. C., 1993.

Blewitt, G., M. B. Heflin, K. J. Hurst, D. C. Jefferson, F. H. Webb and J. F. Zumberge, Absolute far-field displacements from the June 28, 1992, Landers earthquake sequence, *Nature, 361*, 340-342, 1993.

Bock, Y., The use of baseline measurements and geophysical models for the estimation of crustal deformations and the terrestrial reference system, *Rep. 337*, Dep. of Geod. Sci. and Surv., Ohio State Univ., Columbus, 1982.

Bock, Y., Continuous monitoring of crustal deformation, *GPS World, 2 (6)*, 40-47, 1991.

Bock, Y., Crustal deformation and earthquakes, *Geotimes, 39*, 16-18, 1994.

Bock, Y., and S. Shimada, Continuously monitoring GPS networks for deformation measurements, in *Global Positioning System: An Overview*, edited by Y. Bock and N. Leppard, pp. 40-56, Springer Verlag, New York, 1990.

Bock, Y., et al., Continuous monitoring of crustal strain using GPS in southern California, in Proceedings of GPS '90, Second International Symposium on Precise Positioning with the Global Positioning System, edited by D. Delikaraoglou, pp. 853-865, Can. Inst. of Surv. and Mapp., Ottawa, Sept. 3-7, 1990.

Bock, Y., J. Zhang, P. Fang, J. F. Genrich, K. Stark, and S. Wdowinski, One year of daily satellite orbit and polar motion estimation for near real time crustal deformation monitoring, *Developments in Astrometry and their Impact on Astrophysics and Geodynamics, Proc. IAU Symp. 156*, edited by I. I. Mueller and B. Kolaczek, pp. 279-284, Kluwer Acad., Norwell, Mass., 1992.

Bock, Y., et al., Detection of crustal deformation from the Landers earthquake sequence using continuous geodetic measurements, *Nature, 361*, 337-340, 1993a.

Bock, Y., P. Fang, K. Stark, J. Zhang, J. Genrich, S. Wdowinski, and S. Marquez, Scripps Orbit and Permanent Array Center: Report to '93 Bern Workshop, in *Proceedings of 1993 IGS Workshop*, edited by G. Beutler and E. Brockmann, pp. 101-110, Druckerei der Univ. Bern, Bern, Switzerland, 1993b.

Boucher, C., Z. Altamimi, and L. Duhem, Results and analysis of the ITRF93, *IERS Tech. Note 18*, Int. Earth Rotation Serv., Obs. de Paris, 1994.

Bowie, W., Comparison of old and new triangulation data in California, *U.S. Coast Geod. Surv. Spec. Publ. 151*, 1928. (Reprinted in *Reports on Geodetic Measurement of Crustal Movement 1906-1971*, Nat. Geod. Surv., Silver Spring, Md., 1973.)

Bürgmann, R., P. Segall, M. Lisowski, and J. Svarc, Postseismic strain following the 1989 Loma Prieta earthquake from GPS and leveling measurements, *J. Geophys. Res., 102*, 4933-4955, 1997.

Calais, E., and J. B. Minster, GPS detection of ionospheric perturbations following the January 17, 1994, Northridge earthquake, *Geophys. Res. Lett., 22*, 1045-1048, 1995.

Chin, M. (Ed.), *GPS Bulletin, 2*, CSTG GPS Subcomm., Nat. Geod. Surv., Silver Spring, Md., 1989.

Davis, T. L., J. Namson, and R. F. Yerkes, A cross section of the Los Angeles area: Seismically active fold and thrust belt, the 1987 Whittier Narrows earthquake and earthquake hazard, *J. Geophys. Res., 94*, 9644-9664, 1989.

DeMets, C., R. G. Gordon, D. Argus, and S. Stein, Current plate motions, *Geophys. J. Int., 101*, 425-478, 1990.

DeMets, C., R. G. Gordon, D. Argus and S. Stein, Effects of recent revisions to the geomagnetic reversal time scale on estimates of current plate motions, *Geophys. Res. Lett., 21*, 2191-2194, 1994.

Dolan, J. F., K. Sieh, T. K. Rockwell, R. S. Yeats, J. Shaw, J. Suppe, G. J. Huftile, and E. M. Gath, Prospects for larger or more frequent earthquakes in the Los Angeles metropolitan region, *Science, 267*, 199-205, 1995.

Dong, D., and Y. Bock, Global Positioning System network analysis with phase ambiguity resolution applied to crustal deformation studies in California, *J. Geophys. Res., 94*, 3949-3966, 1989.

Donnellan A., B. H. Hager, R. King, and T. Herring, Geodetic measurement of deformation in the Ventura basin region, southern California, *J. Geophys. Res., 98*, 21,727-21,740, 1993.

Dragert H., and R. Hyndman, Continuous GPS monitoring of elastic strain in the northern Cascadia subduction zone, *Geophys. Res. Lett., 22*, 755-759, 1995.

Duan, J., et al., Remote sensing of atmospheric water vapor using the Global Positioning System, *J. Appl. Meteorol., 35*, 830-838, 1996.

Fang, P., and Y. Bock, Scripps Orbit and Permanent Array Center report to the IGS, in *1994 Annual Report, International GPS Service for Geodynamics*, edited by J. F. Zumberge, R. Liu, and R. E. Neilan, pp. 213-233, IGS Cent. Bur., Jet Propul. Labo., Pasadena, Calif., 1995.

Feigl, K. L., et al., Space geodetic measurement of crustal deformation in central and southern California, 1984-1992, *J. Geophys. Res., 98*, 21,677-21,712, 1993.

Freymueller, J., N. E. King, and P. Segall, The co-seismic slip distribution of the Landers earthquake, *Bull. Seismol. Soc. Am., 84*, 646-659, 1994.

Genrich, J. F., and Y. Bock, Rapid resolution of crustal motion at short ranges with the Global Positioning System, *J. Geophys. Res., 97*, 3261-3269, 1992.

Gladwin, M. T., R. L. Gwyther, J. W. Higbie, and R. G. Hart, A medium term precursor to the Loma Prieta earthquake?, *Geophys. Res. Lett., 18*, 1377-1380, 1991.

Gurtner, W., RINEX-The Receiver Independent Exchange Format, *GPS World, 5 (7)*, 1994.

Happer, J., D. Agnew, Y. Bock, H. Johnson, K. Stark, F. Wyatt and D. Jackson, Results from continuous GPS measurements over a 14-km line, *Eos Trans. AGU, 72 (17)*, Spring Meet. Suppl., 118, 1991.

Hayford, J. F., and A. L. Baldwin, The Earth movements in the California earthquake of 1906, in *U.S. Coast and Geodetic Survey Report for 1907*, U.S. Coast and Geod. Surv., Silver Spring, Md., 1907. (Reprinted in *Reports on Geodetic Measurement of Crustal Movement 1906-1971*, Nat. Geod. Surv., Silver Spring, Md, 1973.)

Heki, K., S. Miyazaki, and H. Tsuji, Silent fault slip following an interplate thrust earthquake at the Japan trench, *Nature, 386*, 595-598, 1997.

Herring, T. A., Documentation of the GLOBK Software version 3.3, Mass. Inst. of Technol., Cambridge, 1995.

Herring, T. A., J. L. Davis, and I. I. Shapiro, Geodesy by radio interferometry: The application of Kalman filtering to the analysis of very long baseline interferometry data, *J. Geophys. Res. 95*, 12,561-12,583, 1990.

Hudnut, K. W., et al., Coseismic displacements of the 1992 Landers earthquake sequence, *Bull. Seismol. Soc. Am., 84*, 625-645, 1994.

Hudnut, K. W., et al., Coseismic displacements of the 1994 Northridge, California, earthquake, *Bull. Seismol. Soc. Am.*, S19-S36, 1996.

Ivins, E. R., and C. G. Sammis, Transient creep of a composite lower crust 1. Constitutive theory, *J. Geophys. Res., 101*, 27,981-28,004, 1996.

Ivins, E. R., Transient creep of a composite lower crust 2. A polymineralic basis for rapidly evolving postseismic deformation modes, *J. Geophys. Res., 101*, 27,005-28,028, 1996.

Jaldehag, R. T. K., J. M. Johansson, J. L. Davis, and P. Elósegui, Geodesy using the Swedish permanent GPS network: Effects of snow accumulation on estimates of site positions, *Geophys. Res. Lett., 23*, 1601-1604, 1996.

Johnston, M. J. S., A. T. Linde, and D. C. Agnew, Continuous borehole strain in the San Andreas fault zone before, during, and after the 28 June 1992, M_W 7.3 Landers, California, earthquake, *Bull. Seismol. Soc. Am., 84*, 799-805, 1994.

King, N. E., J. L. Svarc, E. B. Fogleman, W. K. Gross, K. W. Clark, G.

D. Hamilton, C. H. Stiffler, and J. M. Sutton, Continuous GPS observation across the Hayward fault, California, 1991-1994, *J. Geophys. Res., 100,* 20,271-20,284, 1995.

King, R. W., and Y. Bock, Documentation of the GAMIT GPS Analysis Software version 9.3, Mass. Inst. of Technol., Cambridge, 1995.

Langbein J., and H. Johnson, Correlated errors in geodetic time series: Implications for time-dependent deformation, *J. Geophys. Res., 102,* 591-604, 1997.

Langbein, J. O., F. Wyatt, H. Johnson, D. Hamann, and P. Zimmer, Improved stability of a deeply anchored geodetic monument for deformation monitoring, *Geophys. Res. Lett., 22,* 3533-3536, 1995.

Larsen, S., Crustal deformation on southern California, Ph.D. thesis, Calif. Inst. of Technol., Pasadena, 1990.

Li, V. C., and J. R. Rice, Crustal deformation in great California earthquake cycles, *J. Geophys. Res., 92,* 11,533-11,551, 1987.

Lindqwister, U. J., G. Blewitt, R. B. Henderson, and S. C. Pogorelc, Design and testing of a continuously monitoring GPS-based system, *Eos Trans. AGU, 70,* 1054, 1989.

Lindqwister, U., G. Blewitt, J. Zumberge, and F. Webb, Millimeter-level baseline precision results from the California Permanent GPS Geodetic Array, *Geophys. Res. Lett., 18,* 1135-1138, 1991.

Lindvall, S., and T. Rockwell, Holocene activity of the Rose Canyon fault zone in San Diego California, *J. Geophys. Res., 100,* 24,121-24,146, 1995.

Lisowski, M., J. C. Savage, and W. H. Prescott, The velocity field along the San Andreas fault in central and southern California, *J. Geophys. Res., 93,* 8369-8389, 1991.

Lyzenga, G. A., A. Raefsky, and S. G. Mulligan, Models of recurrent strike-slip earthquake cycles and the state of crustal stress, *J. Geophys. Res., 96,* 21,623-21,640, 1991.

Massonnet, D., M. Rossi, C. Carmona, F. Adragna, G. Peltzer, K. Feigl, and T. Rabaute, The displacement field of the Landers earthquake mapped by radar interferometry, *Nature, 364,* 138-142, 1993.

Massonnet, D., K. Feigl. M. Rossi, and F. Adragna, Radar interferometric mapping of deformation in the year after the Landers earthquake, *Nature, 369,* 227-230, 1994.

Massonnet, D., K. Feigl, H. Vadon, and M. Rossi, Coseismic deformation field of the M=6.7 Northridge, California, earthquake of January 17, 1994 recorded by two radar satellites using interferometry, *Geophys. Res. Lett., 23,* 969-972, 1996a.

Massonnet, D., W. Thatcher, and H. Vadon, Detection of postseismic fault-zone collapse following the Landers earthquake, *Nature, 382,* 612-616, 1996b.

Miller, M. M., F. H. Webb, D. Townsend, M. P. Golombek, and R. K. Dokka, Regional coseismic deformation from the June 28, 1992, Landers, California, earthquake: Results from the Mojave GPS network, *Geology, 21,* 868-872, 1993.

Minster, B., et al., Report of the plate motion and deformation panel, paper presented at NASA Coolfont Workshop, Coolfont, W. Va., August, 1989.

Minster, J. B., B. H. Hager, W. H. Prescott and R. E. Schutz, International global network of fiducial stations, report U.S. Natl. Res. Counc., Natl. Acad. Press, Washington, D. C., 1991.

Müller, J. J. A., De Verplaatsing van Eeenige Triangulatie-Pilaren in de Residentie Tapanoeli (Sumatra) tengevolge van dc aardbeving van 17 Mei 1892, *Ver. der Koninkl. Akad. Wet. Amsterdam, III (2),* 1895.

Murakami, M., M. Tobita, S. Fujiwara, T. Saito, and H. Masaharu, Coseismic crustal deformations of 1994 Northridge, California, earthquake detected by interferometric JERS 1 synthetic aperture radar, *J. Geophys. Res., 101,* 8605-8614, 1996.

Namson, J., and T. Davis, Structural transect of the western Transverse Ranges, California: Implications for lithospheric kinematics and seismic risk evaluation, *Geology, 16,* 675-679, 1988.

Okada, Y., and E. Yamamoto, Dyke intrusion model for the 1989 seismo-volcanic activity off Ito, central Japan, *J. Geophys. Res., 96,* 10,361-10,376, 1991.

Oral, M. B., Global Positioning System (GPS) measurements in Turkey (1988-1992): Kinematics of the Africa-Arabia-Eurasia plate collision zone, Ph.D. thesis, Mass. Inst. of Technol., Cambridge, 1994.

Peltzer, G., P. Rosen, F. Rogez, and K. Hudnut, Postseismic rebound in fault step-overs caused by pore fluid flow, *Science, 273,* 1202-1204, 1996.

Prescott, W. H., Satellites and earthquakes: A new continuous GPS array for Los Angeles, Yes, It will radically improve seismic risk assessment for Los Angeles, *Eos Trans. AGU, 77,* 417, 1996.

Reches, Z., G. Schubert, and C. Anderson, Modeling of periodic great earthquakes on the San Andreas fault: Effects of nonlinear crustal rheology, *J. Geophys. Res.,* 99, 21,983-22,000, 1994.

Reid, H. F., The mechanics of the earthquake, in *The California earthquake of April 18, 1906, Report of the State Earthquake Investigation Commission,* vol. 2, *Carnegie Inst. Publ. 87,* 192 pp., 1910. (Reprinted, 1969.)

Reid, H. F., Sudden Earth movements in Sumatra, *Bull. Seismol. Soc. Am., 3,* 72-79, 1913.

Ryan, J. W., C. Ma, and D. S. Caprette, NASA Space Geodesy Program — GSFC Data Analysis — 1992, *NASA Tech. Memo. TM 104572,* 1993.

Savage, J. C., Principal component analysis of interseismic deformation in southern California, *J. Geophys. Res., 100,* 12,691-12,701, 1995.

Savage, J. C., and M. Lisowski, Interseismic deformation along the San Andreas fault in southern California, *J. Geophys. Res., 100,* 12,703-12,717, 1995a.

Savage, J. C., and M. Lisowski, Changes in long-term extension rates associated with the Morgan Hill and Loma Prieta earthquakes in California, *Geophys. Res. Lett., 22,* 759-762, 1995b.

Savage, J. C., and J. L. Svarc, Postseismic deformation associated with the 1992 M_W=7.3 Landers earthquake, southern California, *J. Geophys. Res., 102,* 7565-7577, 1997.

Savage, J. C., W. H. Prescott, M. Lisowski, and N. King, Deformation across the Salton trough, California, 1973-1977, *J. Geophys. Res., 84,* 3069-3079, 1979.

Savage, J. C., W. H. Prescott, and G. Gu, Strain accumulation in southern California, 1973-1984, *J. Geophys. Res., 91,* 7455-7473, 1986.

Savage J. C. , M. Lisowski, and W. H. Prescott, An apparent shear zone trending north-northwest across the Mojave desert into Owens Valley, eastern California, *Geophys. Res. Lett., 17,* 2113-2116, 1990.

Savage, J. C., M. Lisowski, and J. L. Svarc, Postseismic deformation following the 1989 (M=7.1) Loma Prieta, California, earthquake, *J. Geophys. Res., 99,* 13,757-13,765, 1994.

Scholz, C. H., *The Mechanics of Earthquakes and Faulting,* Cambridge Univ. Press, New York, 1990.

Schupler, B. R., R. L. Allhouse, and T. A. Clark, Signal characteristics of GPS user antennas, *Navigation, 41,* 277-295, 1994.

Shen, Z-K., D. D. Jackson, Y. Feng, M. Cline, M. Kim, P. Fang and Y. Bock, Postseismic deformation following the Landers earthquake, California, June 28, 1992, *Bull. Seismol. Soc. Am., 84,* 780-791, 1994.

Shen, Z.-K., D. D. Jackson, and X. B. Ge, Crustal deformation across and beyond the Los Angeles basin from geodetic measurements, *J. Geophys. Res., 101,* 27,957-27,980, 1996.

Shimada, S., and Y. Bock, Crustal deformation measurements in Central Japan determined by a GPS fixed-point network, *J. Geophys. Res., 97,* 12,437-12,455, 1992.

Shimada, S., S. Sekiguchi, T. Eguchi, Y. Okada, and Y. Fujinawa, Preliminary results of the observation by fixed-point GPS simultaneous baseline determination network in Kanto-Tokai district, *J. Geod. Soc. Jpn., 35,* 85-95, 1989.

Shimada S., Y. Fujinawa, S. Sekiguchi, S. Ohmi, T. Eguchi, and Y. Okada, Detection of a volcanic fracture opening in Japan using Global Positioning System measurements, *Nature, 343,* 631-633, 1990.

SOPAC Staff, Scripps Orbit and Permanent Array Center and Southern California Permanent GPS Geodetic Array, in *Proceedings of National Research Council,* Natl. Res. Counc., Washington, D.C., in press, 1997.

Thatcher, W., Horizontal deformation measurements from historic geodetic measurements in southern California, *J. Geophys. Res.,* 84, 2351-2370, 1979.

Thatcher, W., Nonlinear strain buildup and the earthquake cycle on the San Andreas fault, *J. Geophys. Res.,* 88, 5893-5902, 1983.

Thatcher, W., The earthquake deformation cycle, recurrence, and the time-predictable model, *J. Geophys. Res.,* 849, 5674-5680, 1984.

Thomas, J. B., Functional description of signal processing in the Rogue GPS receiver, *JPL Publ. 88-15,* 1988.

Tsuji, H., Y. Hatanaka, T. Sagiya and M. Hashimo, Coseismic crustal deformation from the 1994 Hokkaido-Toho-Oki earthquake monitored by a nationwide continuous GPS array in Japan, *Geophys. Res. Lett., 22,* 1669-1673, 1995.

Ward, S. N., Pacific-North America plate motions: New results from very long baseline interferometry, *J. Geophys. Res., 95,* 21,965-21,981, 1990.

Wdowinski, S., Y. Bock, P. Fang, J. F. Genrich, D. C. Agnew and F. K. Wyatt, The 1992 Landers earthquake sequence: Detection of

coseismic and postseismic surface displacement, *Eos Trans. AGU, 73 (43)*, Fall. Meet. Suppl., 364, 1992.

Wdowinski, S., Y. Bock, J. Zhang, P. Fang, and J. F. Genrich, Southern California Permanent GPS Geodetic Array: Spatial filtering of daily positions for estimating coseismic and postseismic displacements induced by the 1992 Landers earthquake, J. Geophys. Res., this issue.

Wessel, P., and W. H. F. Smith, Free software helps map and display data, *Eos Trans. AGU, 72*, 445-446, 1991.

Whitten, C. A., Measurements of Earth movements in California, *Calif. Div. Mines Bull., 171*, 75-80, 1955. (Reprinted in *Reports on Geodetic Measurement of Crustal Movement 1906-1971*, Nat. Geod. Surv., Silver Spring, Md, 1973.)

Working Group on California Earthquake Probabilities, Seismic hazards in southern California — Probable earthquakes, 1994 to 2024, *Bull. Seismol. Soc. Am. , 85*, 379-439, 1995.

Wyatt, F. K., H. Bolton, S. Bralla, and D. C. Agnew, New designs of geodetic monuments for use with GPS, *Eos Trans. AGU, 70*, 1054-1055, 1989.

Wyatt, F. K., D. C. Agnew, and M. Gladwin, Continuous measurements of crustal deformation for the 1992 Landers earthquake sequence, *Bull. Seismol. Soc. Am. 84*, 768-779, 1994.

Zebker, H. A., P. A. Rosen, and R. M. Goldstein, On the derivation of coseismic displacement fields using differential radar interferometry: The Landers earthquake, *J. Geophys. Res., 99*, 19,617-19,634, 1994.

Zhang, J., Continuous GPS measurements of crustal deformation in southern California, Ph.D. dissertation, Univ. of Calif., San Diego, 1996.

Zhang, J., Y. Bock, H. Johnson, P. Fang, J. Genrich, S. Williams, S. Wdowinski, and J. Behr, Southern California Permanent GPS Geodetic Array: Error analysis of daily position estimates and site velocities, *J. Geophys. Res.*, this issue.

D. Agnew, J. Behr, Y. Bock, J. Dean, M. van Domselaar, P. Fang, J. Genrich, H. Johnson, B. Oral, K. Stark, S. Williams, F. Wyatt and J. Zhang, Cecil H. and Ida M. Green Institute of Geophysics and Planetary Physics, Scripps Institution of Oceanography, 9500 Gilman Drive, La Jolla, CA 92093-0225. (email: dagnew@ucsd.edu; behr@gps.caltech.edu; ybock@ucsd.edu; jdean@pgga.ucsd.edu; matthijs@pgga.ucsd.edu; pfang@pgga.ucsd.edu; jeff@pgga.ucsd.edu; johnson@ramsden.ucsd.edu; burcoral@alum.mit.edu; stark@dukester.com; simon@pgga.ucsd.edu; wyatt@ramsden.ucsd.edu; jie@illustra.com)

S. Dinardo, Jet Propulsion Laboratory, 4800 Oak Grove Drive, Pasadena, CA 91109. (sjd@logos.jpl.nasa.gov)

W. Gurtner, Astronomical Institute, University of Bern, Sidlerstrasse 5, CH-3012, Bern, Switzerland. (gurtner@aiub.unibe.ch)

T. Herring and R. King, Department of Earth, Atmospheric, and Planetary Sciences, Massachusetts Institute of Technology, 77 Massachusetts Avenue, Cambridge, MA 02139. (tah@prey.mit.edu; rwk@chandler.mit.edu)

K. Hudnut, U.S. Geological Survey, 525 South Wilson, Pasadena, CA 91106. (hudnut@seismo.gps.caltech.edu)

D. Jackson, Department of Earth and Space Sciences, University of California Los Angeles, 405 Hilgard Ave., Los Angeles, CA 90024. (jackson@cyclop.ess.ucla.edu)

S. Wdowinski, Department of Geophysics and Planetary Physics, Tel Aviv University, Ramat Aviv, 69978 Israel. (shimon@geol.tau.ac.il)

W. Young, Riverside County Flood and Water Conservation District, P.O. Box 1033, Riverside, CA 92502. (byoung@deltanet.com)

(Received October 22, 1996; revised April 25, 1997;
accepted May 6, 1997.)